Laboratory Experiments on Bentonite Samples: FY15 Progress

Fuel Cycle Research & Development

Revision 2
12/20/2012

APPENDIX E

FCT DOCUMENT COVER SHEET [1]

Name/Title of
Deliverable/Milestone/Revision No. Laboratory Experiments on Bentonite Samples: FY15 Progress

Work Package Title and Number DR Crystalline Disposal R&D – LBNL FT-15LB080704

Work Package WBS Number 1.02.08.07

Responsible Work Package Manager Jim Houseworth   (Signature on File)

(Name/Signature)

Date Submitted   7/24/2015

Quality Rigor Level for Deliverable/Milestone[2]	☒ QRL-3	☐ QRL-2	☐ QRL-1 ☐ Nuclear Data	☐ Lab/Participant QA Program (no additional FCT QA requirements)

This deliverable was prepared in accordance with   Lawrence Berkeley National Laboratory

(Participant/National Laboratory Name)

QA program which meets the requirements of
☒ DOE Order 414.1   ☐ NQA-1-2000   ☐ Other

This Deliverable was subjected to:

☒ Technical Review   ☐ Peer Review

Technical Review (TR)   **Peer Review (PR)**

Review Documentation Provided   **Review Documentation Provided**

☐ Signed TR Report or,   ☐ Signed PR Report or,

☐ Signed TR Concurrence Sheet or,   ☐ Signed PR Concurrence Sheet or,

☐ Signature of TR Reviewer(s) below   ☐ Signature of PR Reviewer(s) below

Name and Signature of Reviewers

Jim Houseworth   (Signature on File)

NOTE 1: *Appendix E should be filled out and submitted with the deliverable. Or, if the PICS:NE system permits, completely enter all applicable information in the PICS:NE Deliverable Form. The requirement is to ensure that all applicable information is entered either in the PICS:NE system or by using the FCT Document Cover Sheet.*

NOTE 2: *In some cases there may be a milestone where an item is being fabricated, maintenance is being performed on a facility, or a document is being issued through a formal document control process where it specifically calls out a formal review of the document. In these cases, documentation (e.g., inspection report, maintenance request, work planning package documentation or the documented review of the issued document through the document control process) of the completion of the activity along with the Document Cover Sheet is sufficient to demonstrate achieving the milestone. If QRL 1, 2, or 3 is not assigned, then the Lab/Participant QA Program (no additional FCT QA requirements box must be checked, and the work is understood to be performed, and any deliverable developed, in conformance with the respective National Laboratory/Participant, DOE- or NNSA-approved QA Program.*

This page is intentionally blank.

TABLE OF CONTENTS

LIST OF FIGURES

ACRONYMS

EBS	Engineered Barrier Systems
EDL	Electric Double Layer
DIS	Diffuse Ion Swarm
HLRW	High Level Radioactive Waste
HTO	Tritiated Water
IAEA	International Atomic Energy Agency
LBNL	Lawrence Berkeley National Laboratory
NEA, OECD	Nuclear Energy Agency, Organisation for Economic Co-operation and Development
TIC	Total Inorganic Carbon
MD	Molecular Dynamics
TDS	Total Dissolved Solids

This page is intentionally blank.

PROJECT SUMMARY

The development of performance assessment models for long-term nuclear waste storage facilities requires a systematic understanding of the underlying processes of radioactive contaminant release and transport behavior. The potential mobility of uranium(VI) is especially important, because uranium is the primary component of the nuclear fuel matrix, and the release of other radioisotopes will be controlled by the dissolution and diffusive transport rates of uranium(VI) away from the source term. Bentonite and clays have been proposed as backfill materials in Engineered Barrier Systems (EBS) in close contact with waste containers, or as host rock media in many high-level radioactive waste storage programs worldwide. A realistic conceptual understanding of diffusive transport of uranium(VI) in clays and bentonite is therefore essential for the development of performance assessment models with accurate predictive capabilities. In this context, uranium(VI) sorption onto bentonite and sodium-montmorillonite, its major mineralogical component, is an important, and potentially limiting process affecting uranium(VI) fluxes and contaminant retardation. Hence, the primary goal of this study is to provide a fundamental understanding of uranium(VI) sorption and transport behavior in Na-montmorillonite and bentonite.

Across the EBS and as a function of time, gradients are to be expected with regard to chemical solution conditions (e.g., pH, calcium and bicarbonate concentrations, etc.) and temperature. These gradients can be caused by the presence of calcite impurities in the bentonite buffer, the vicinity of the EBS to concrete barriers and radiation heat released by nuclear waste packages. Changes in these parameters can dramatically affect uranium(VI) solution speciation, the type of clay surface sites predominantly involved in uranium(VI) sorption reactions, the diffusion-accessible porosity for uranium(VI) species, and the mineral and surface characteristics of the solids due to heat-induced mineral alterations. All of these factors are expected to lead to secondary effects on uranium(VI) sorption and diffusion characteristics. Hence, a realistic conceptual model describing uranium(VI) mobility needs to incorporate these relationships in order to capture uranium(VI) mobility over time and space in the future repository. Therefore, as a secondary goal, we are investigating uranium(VI) sorption and diffusion behavior as a function of chemical solution conditions and after heat-induced mineral alterations.

Given these research needs, the primary research goals for this study and for this fiscal year are as follows:

- Evaluate the potential effects of heat-induced mineral alterations in bentonite on uranium(VI) sorption behavior in batch experiments;
- Perform a uranium(VI) through-diffusion experiment to investigate the relevance of full or partial anion-exclusion of uranium(VI) species from Na-montmorillonite interlayer spaces, under alkaline pH conditions.
- Determine uranium(VI) diffusion coefficients in Na-montmorillonite (in the absence of Ca concentration levels affecting uranium(VI) speciation) for their later use in performance assessment models.
- Evaluate effects of uranium(VI) surface complexation reactions on its diffusive transport behavior.
- Demonstrate a successful experimental approach for uranium(VI) through-diffusion experiments, while providing experimental data needed for performance assessment.

Experimental results from uranium(VI) sorption experiments with bentonite samples before and after heat treatments suggest a decrease in uranium(VI) sorption due to heat-induced mineral alterations. This effect could lead to lower uranium(VI) retardation in comparison to the pristine solids, and potential changes in diffusive uranium(VI) fluxes.

Current results from parallel uranium(VI) through-diffusion experiments in Na-montmorillonite at two, slightly different, alkaline pH conditions (pH 8.75 and 8.95), indicate a relevance of so-called anion exclusion effects, the full or partial exclusion of anionic uranium(VI) solution species from clay interlayer spaces. Such exclusion affects the diffusion-accessible porosity for uranium(VI) species predominant under these chemical solution conditions, as well as the resulting uranium(VI) diffusive fluxes. Based on the literature we have reviewed, this is the first time this phenomenon has been experimentally demonstrated in a through-diffusion experiment. Hence, this result will have a profound impact on conceptual models describing the diffusive transport behavior of uranium(VI) in montmorillonite and bentonite.

Also, uranium(VI) sorption reactions were shown to be relevant for contaminant retardation in diffusion experiments, even at alkaline pH values of pH 8.75 and 8.95, where uranium(VI) sorption is low compared to other pH conditions. Despite the similarity of these pH conditions in the parallel diffusion experiments, different degrees of uranium(VI) retardation could be observed in the two systems. Additionally, we also observed different, apparent kinetic limitations for uranium(VI) sorption reactions as a function of pH, which was indicated by varying time-frames required to reach steady-state conditions for uranium diffusive fluxes. The latter suggests that the kinetic limitations for one or more reaction step(s) in the overall sorption process are dependent on chemical solution conditions, e.g., as could be the case, for instance, for a rate-limited dissociation of uranium(VI) solution complexes prior to the formation of uranium(VI) surface complexes.

All of these results, as well as the series of experimentally-determined uranium(VI) sorption and diffusion parameters, support the development of realistic conceptual models describing uranium(VI) mobility in nuclear waste repositories, and provide direct input parameters for performance assessment models.

1. INTRODUCTION AND RESEARCH MOTIVATION

Nuclear fission produces 14% of the world's electricity supply and could contribute ~15% of CO_2 abatement efforts required to stabilize global CO_2 emissions over the next 50 years (Pacala and Socolow, 2004; Englert et al., 2012). The viability of nuclear energy as a CO_2 abatement technology, however, relies in part on the demonstration that geologic storage facilities can isolate high level radioactive waste (HLRW) on time scales commensurate with the decay of long-lived radioactive fission products and actinides, on the order of 10^6 years. Accurate predictions of repository performance on such long time scales require the development of geophysical models grounded in fundamental knowledge of material properties and constitutive relationships relevant to radionuclide migration in geologic media (Altmann et al., 2012). Depending on the perspective, the radioelements of greatest concern in HLRW storage are those that are present in high abundance (such as uranium), those that are large contributors to the long-term radiotoxic inventory [such as plutonium, americium, curium and neptunium (Kaszuba and Runde, 1999; IAEA, 2004)], or those that have a long half-life and a significant solubility in water: ^{129}I, ^{36}Cl, ^{79}Se, ^{99}Tc, ^{126}Sn, and ^{135}Cs (Altmann, 2008; NEA, 2009).

Most countries with HLRW storage programs are currently investigating clayey media, such as bentonite and shale, for use as engineered barrier systems (EBS) and/or host rocks of geologic repositories (ANDRA, 2005; Delay et al., 2007; Altmann, 2008; Guyonnet et al., 2009; Bock et al., 2010; SKB, 2011; Altmann et al., 2012). At the conditions that would exist in proposed HLRW repositories, clay barriers display very low hydraulic conductivities, the ability to self-seal when fractured, and water and solute mass fluxes that are dominated by molecular diffusion as the primary transport mechanism on time-scales of millions of years (Neuzil, 1986, 1994, 2013; Horseman and Volckaert, 1996; Oscarson et al., 1996; Bock et al., 2010; Mazurek et al., 2011).

Sodium-montmorillonite, the main constituent of bentonite, is a smectite, a 2:1-layer-type dioctahedral phyllosilicate with a large specific surface area (~800 m^2 g^{-1}) and cation exchange capacity (~1 mmol g^{-1}). Each clay layer has a thickness of ~1 nm and carries negatively-charged isomorphic substitutions in its phyllosilicate framework. The aggregation of Na-montmorillonite layers into particles (i.e., stacks of clay layers) results in a complex pore-size distribution including narrow (~1 nm wide) interlayer pores within particles (where diffusion is strongly impacted by clay surfaces) and larger pores between particles (where water may be bulk-liquid-like). Furthermore, Na-montmorillonite provides reactive surface sites for radionuclide sorption reactions, primarily in two forms: (1) cation exchange sites on the planar surfaces of clay layers and (2) surface complexation sites in the form of amphoteric octahedral Al-OH and tetrahedral Si-OH sites on the edges of clay layers making up clay particles. The relevance of a particular type of surface site for contaminant sorption and retardation is strongly dependent on the chemical solution conditions (e.g. ionic strength) and contaminant solution speciation (e.g. with regard to cationic, anionic and neutral species, in a given system).

The diffusion coefficients of water and solutes in clayey media have been extensively studied in conditions relevant to HLRW repositories, particularly in the case of water tracers (HTO), anions (I^-, Br^-, Cl^-, TcO_4^-, SeO_3^{2-}), and alkali and alkaline earth metals (Na^+, Cs^+, Ca^{2+}, Sr^{2+}) (Muurinen et al., 1986; Sato et al., 1992; Kozaki et al., 1996, 1998a; b; Choi and Oscarson, 1996; Kozaki et al., 1999a; b, 2001, 2005, 2008, 2010; Lee et al., 1996; Nakajima et al., 1997; Nakashima, 2000, 2002, 2003, 2006; Molera, 2002; Molera and Eriksen, 2002; Molera et al., 2003; Sato and

Suzuki, 2003; Van Loon et al., 2003a; b, 2004a; b, 2005a; b, 2007; Wang, 2003; Jansson and Eriksen, 2004; García-Gutiérrez et al., 2004; Sato and Miyamoto, 2004; Suzuki et al., 2004; García-Gutiérrez et al., 2009; Wang and Liu, 2004; Wang and Tao, 2004; Melkior et al., 2005, 2007, 2009; Nakashima and Mitsumori, 2005; Wang et al., 2005; Appelo and Wersin, 2007; Glaus et al., 2011, 2013; Motellier et al., 2007; Glaus et al., 2007, 2008, 2010; Gonzàlez Sànchez et al., 2008; Descostes et al., 2008; Wersin et al., 2008; Wittebroodt et al., 2008; Jakob et al., 2009; Jougnot et al., 2009; Appelo et al., 2010; Savoye et al., 2010, 2011; Holmboe et al., 2011; Gimmi and Kosakowski, 2011; Loomer et al., 2013; Tachi and Yotsuji, 2014). In comparison, uranium and other strongly-sorbing actinides have been studied less extensively (Bai et al., 2009; F; García-Gutiérrez et al., 2003; Joseph et al., 2013; Korichi et al., 2010; Liu et al., 2010; Maes et al., 2002; Muurinen, 1990; Pekala et al., 2009, 2010; Tokunaga et al., 2004) with regards to their diffusive transport behavior in clayey media for a wide range of chemical conditions. Nevertheless, as the basis of nuclear fuel, uranium is one of the primary elements to be considered in environmental risk assessments for nuclear waste repositories. Other radionuclides that are bound in the fuel matrix can only be released at the same rate as uranium dissolves and diffuses through waste containment barriers (Muurinen, 1990). Furthermore, in conceptual studies uranium can serve as a useful analog for other radioactive contaminants, such as Pu, Np, and Am, due to its sorption characteristics, the relevance of uranium-carbonate species for actinide speciation, and the availability of a well-established thermodynamic database describing uranium solution speciation at various chemical conditions. Hence, the characterization of uranium(VI) sorption and diffusion behavior in sodium-montmorillonite and bentonite is the primary focus of this study.

The complexity of the mineralogical structure of montmorillonite, in terms of (1) its pore-size distributions and (2) available surface site types, has important implications for the diffusive transport of radionuclides in bentonite barriers. First, the 'co-existence' of small interlayer pores within particles and larger macropores between clay particles can create two types of clay porosities and diffusion pathways. The relevance of the individual porosities and pathways is strongly dependent on system characteristics, such as the degree of bentonite compaction, chemical solution conditions, and the charge of contaminant species in solution. For instance, a partial or full exclusion of anions from negatively charged clay interlayer spaces can change the effective 'anion-accessible' porosity and decrease the diffusive flux of these solutes under steady state conditions. As a result, diffusive fluxes can vary substantially between cations, anions and uncharged solutes. Furthermore, radionuclides that show dramatic changes in their chemical solution speciation as a function of pH, such as uranium, and are able to form cationic, anionic or uncharged species in solution, are expected to show different diffusive transport behavior under varying chemical solution conditions.

Second, montmorillonite surface site characteristics, and radionuclide sorption affinities for clay surfaces have important implications for diffusive transport as well. While any type of surface reaction results in a retardation of the radionuclide relative to a non-reactive tracer, weak and strong surface reactions can have different net effects on diffusive fluxes under steady state conditions. In case of weak cation exchange reactions, adsorbed cations show a significant mobility in the electric double layer (EDL) (Jenny and Overstreet, 1939; Van Schaik et al., 1966; Nye, 1980; Jakob et al., 2009; Gimmi and Kosakowski, 2011), because of the high, local concentration gradients along the surface. This mobility leads to a 'surface diffusion' of adsorbed cations, in addition to their diffusion in the liquid phase, which, in turn, results in higher total

diffusive fluxes under steady state conditions. In contrast, strong sorption reactions, e.g. in the form of surface complexation reactions on edge sites, do not contribute significantly to surface diffusion fluxes under steady state conditions. As a result, the distribution of clay surface sites further complicates the prediction of diffusive fluxes for radionuclides that show substantially different chemical solution speciation as a function of pH. For instance, at low pH conditions, uranium(VI) may be predominantly present as cationic species, sorb onto clay via (potentially weak) cation exchange reactions, and may not be affected by anion exclusion effects. This could cause retardation of uranium(VI) diffusion relative to a non-reactive tracer, but possibly higher diffusive uranium(VI) fluxes compared to the non-reactive tracer or to uranium(VI) diffusion at higher pH conditions. At more alkaline pH, where uranium(VI) is present as anionic species, uranium(VI) is expected to sorb onto montmorillonite in the form of (potentially strong) surface complexation reactions, and be subject to full or partial anion exclusion from clay interlayer spaces. In this case, uranium(VI) retardation may be coupled with comparable or lower diffusive fluxes relative to non-reactive tracers.

Based on the literature we have reviewed, at present full or partial anion exclusion effects have not been clearly demonstrated experimentally for anionic uranium(VI) species, despite the theoretical understanding of the uranium(VI)-montmorillonite system described above. This is, at least in part, due to the difficulties associated with the experimental approach of so-called uranium(VI) through-diffusion experiments, which monitor the breakthrough and diffusive fluxes of uranium(VI) across a diffusion cell over the course of an experiment. Almost all previously reported uranium(VI)-montmorillonite/bentonite diffusion experiments were based on an evaluation of total uranium(VI) concentrations (dissolved plus sorbed concentrations) as a function of distance in the clay packing after the completion of experiments. While this approach still allows determining apparent uranium diffusion coefficients and sorption distribution coefficients (K_d values) based on the simulation of the concentration profile, the associated model parameters are less constrained, and direct observations of solute retardation, diffusive fluxes, and any potential kinetic effects are not possible. Hence, one of our research goals was to demonstrate that uranium(VI) through-diffusion experiments could be conducted successfully under alkaline conditions.

Furthermore, it should be noted that waste forms, and possibly the presence of concrete in the vicinity of an engineered barrier system (EBS), are likely to create alkaline conditions and concentration gradients in chemical variables (pH, HCO_3^-, Ca^{2+}) within the EBS (Figure 1). Hence, it is important to develop conceptual models that can describe uranium(VI) diffusion as a function of chemical solution conditions. Furthermore, an understanding of diffusion rates is needed not only for relevant radionuclides but also predominant earth metals, because the latter elements can affect actinide solution speciation and compete with radionuclides for mineral surface sites. For instance, within engineered clay barriers containing minor amounts of calcite, $Ca_2UO_2(CO_3)_3^0$ is expected to dominate uranium(VI) solution speciation, and hence, control uranium(VI) sorption and diffusion behavior (Kerisit and Liu, 2010; Bradbury and Baeyens, 2011; Joseph et al., 2011). Hence, in an earlier part of this study, we also investigated calcium diffusion behavior in sodium-montmorillonite.

In addition to chemical gradients, gradients in temperature also have to be expected as a function of time and space in the EBS, given the radiation heat produced by the decay of radioactive waste. Besides other factors, an exposure of bentonite and montmorillonite to heat may lead to mineral alterations of the solids, and a possible 'illitization' of montmorillonite, over time

(Cheshire et al., 2014; and references therein). Due to the strong dependency of uranium(VI) sorption and diffusion behavior on solid phase characteristics, this creates a strong research need to investigate the potential effects of mineral alterations in bentonite on uranium(VI) sorption/diffusion behavior. For instance, if uranium(VI) sorption affinities to the solids were different for altered than the original minerals, then uranium(VI) transport behavior would be affected by these heat-induced mineral alterations even after EBS temperatures have returned to their original levels.
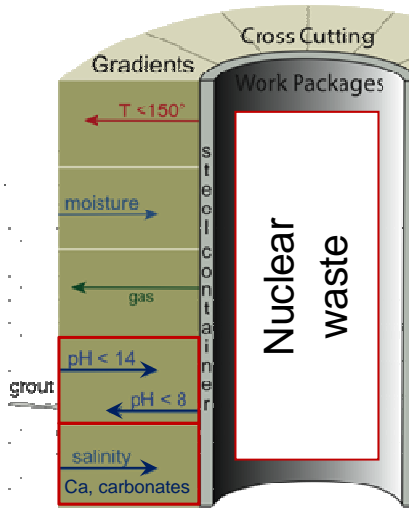
Figure 1. Expected gradients in chemical conditions and temperature across the EBS
            (Modified after http://www.eng.ox.ac.uk/about-us/jobs/fp/THMC.png/image_preview).

Given these research needs, we can summarize the primary research goals for this study for this fiscal year as follows:

- Evaluate the potential effects of heat-induced mineral alterations in bentonite on uranium(VI) sorption behavior in batch experiments;
- Perform a uranium(VI) through-diffusion experiment to investigate the relevance of full or partial anion-exclusion of uranium(VI) species from Na-montmorillonite interlayer spaces, under alkaline pH conditions.
- Determine uranium(VI) diffusion coefficients in Na-montmorillonite (in the absence of Ca concentration levels affecting uranium(VI) speciation) for their later use in performance assessment models.
- Evaluate effects of uranium(VI) surface complexation reactions on its diffusive transport behavior.
- Demonstrate a successful experimental approach for uranium(VI) through-diffusion experiments, while providing experimental data needed for performance assessment.

2.   URANIUM(VI) SORPTION EXPERIMENTS

2.1   Overview and Goals

Previously, we have performed a series of batch sorption envelope experiments in order to investigate the sorption of uranium(VI) to Na-montmorillonite over a range of chemical solution conditions (pH, calcium and carbonate concentrations, as well as total uranium(VI) concentrations). These data sets are currently used to develop a surface complexation model for this system, which will provide a detailed understanding of uranium(VI)-montmorillonite surface interactions.

For this fiscal year, our goal was to investigate potential impacts of heat-induced mineral alterations in bentonite on uranium(VI) sorption behavior, using previous Na-montmorillonite data as a reference. For this purpose, we obtained 'cooked' and 'uncooked' bentonite samples from Dr. Florie Caporuscio's research group at Los Alamos National Laboratory. The resulting experimental data will be useful for diffusion and performance assessment models.

2.2   Materials

All chemicals used in this study were reagent grade or better. Uranium(VI) solutions contained ^{238}U from a 3.7×10^{-4} M uranyl nitrate stock solution (dilution of 1000 μg/mL Inorganic Ventures ICP-MS Standard). Acids, bases, and salt solutions used in equilibrium and kinetic batch experiments were of TraceSelect grade (Sigma Aldrich) in order to minimize calcium background concentrations. Aqueous solutions were prepared with Nanopure water (Barnstead ultrapure water system). Glassware was cleaned by soaking in acid (10 % (v/v) HCl) for 12 to 24 hours, followed by thorough rinsing with Nanopure water and air-drying.

Three types of solids were compared as reactive surfaces for uranium(VI) sorption reactions, 'cooked' and 'uncooked' bentonite and Na-montmorillonite. 'Cooked' and 'uncooked' bentonite samples were provided by Dr. Florie Caporuscio at Los Alamos National Laboratory. The starting bentonite, used in this heat-treatment, was mined from a reducing horizon in Colony, Wyoming, and represents a Na-montmorillonite with minor amounts of clinoptilolite, feldspars, biotite, cristobalite, quartz and pyrite (Caporuscio et al., 2013; Table 3). This material was exposed to a temperature of 300 °C and a pressure of 150-160 bar for 7 weeks (pH of 6.74, solid-liquid ratio of 5:1). For this heat-treatment, the original composition of the brine in contact with the bentonite contained various concentrations of Ca, Cl, K, Na, Si, sulfate and Sr with a Total Dissolved Solids (TDS) content of 1934 mg/L (Caporuscio et al., 2014; Table 1). Redox conditions were buffered during heat-treatment using a Fe_3O_4-Fe^0 buffer system. An extended mineralogical characterization of the solids before and after heat-treatments allowed for the following conclusions. The post-reaction sample (EBS-12) contained lower fractions of clinoptilolite (13% before, 4% after), pyrite (0.4% before, detected but below quantification limit after) and biotite (3% before, detected but below quantification limit after) than the starting material. At the same time, montmorillonite (72% before, 71% after) and feldspar (9% before, 10% after) fractions remained relatively unchanged (Caporuscio et al., 2013; Table 3). Overall, no 'illitization' of montmorillonite was determined, but the formation of new, amorphous phases was observed, especially the formation of analcime at a fraction of 1% or greater. Both the heat-treated ('cooked' bentonite) and starting material ('uncooked' bentonite) were ground with a

Retsch MM 400 ball mill (frequency of 30/sec for 2 minutes) prior to uranium(VI) sorption experiments.

Purified Na-montmorillonite (SWy-2, Clay Minerals Society) served as a reference material for a comparison of uranium(VI) sorption data after 2 days of sorption equilibration. A detailed description of the Na-montmorillonite purification procedure has been provided previously (Rutqvist et al., 2012; Davis et al., 2013). Briefly, pretreatment steps included: the removal of calcite impurities using a 1 M sodium acetate/glacial acetic acid solution (0.564 M) at pH 5; clay equilibration with a 1 M sodium chloride solution; removal of excess salts with Nanopure water; separation of quartz and feldspar impurities from the <2 μm clay fraction by centrifugation; and oven-drying of the purified clay at 45 °C. This purification procedure allowed us to keep calcium background concentrations at or below 88.1 μg/l in the reservoir solutions during the calcium bromide through-diffusion experiment, with a contribution of 33.2 μg/L from the background electrolyte itself. (An evaluation of calcium background concentrations for the uranium(VI) through-diffusion experiments is currently ongoing.)

For each solid, a stock suspension of approximately 10 or 20 g/L solids was prepared in Nanopure water, and its exact solid concentration determined by weighing two 10 mL volume fractions before and after drying at 45 °C. A solid concentration of 0.5 g/L was selected for all batch sorption studies, in order to cover a range of U surface concentrations while avoiding complete (i.e. 100%) uranium(VI) sorption.

2.3   Experimental Procedure

The effect of pH and equilibration time on uranium(VI) sorption behavior was studied in a series of batch sorption experiments with initial pH values of 4, 4.25, 4.5, 4.75, 5, 5.5, 6, 6.5, 7, 7.5, 7.75, 8, 8.25, 8.5, 8.75, and 9, and equilibration times of 2, 6, 11, 15, and 21 days. All batch sorption experiments were conducted at room temperature (22.5 °C - 23.5 °C), with a nominal total uranium(VI) concentration of 10^{-6} M, a solid concentration of 0.5 g/L, and a total ionic strength of 0.1 M NaCl. The main steps of the experiments included: (1) pre-equilibration of the solids with a background electrolyte solution at the specified pH and chemical solution conditions, (2) uranium(VI) sorption equilibration with the mineral phase, (3) time-dependent sampling and analysis of supernatant fractions after removal of the solid phase by centrifugation, and (4) an evaluation of uranium(VI) wall sorption effects based on an acid-wash procedure.

At the beginning of experiments, aliquots of Nanopure water, solid stock suspensions and a 1M NaCl solution were transferred into sample vials ('50-mL' polycarbonate Oakridge centrifuge tubes) to give the desired solid concentration and ionic strength in the final sample volume of 40 mL. For samples with target pH values of ≥ 7.0, increasing amounts of 1M or 0.1M NaHCO$_3$ buffer solutions were added. Solution pH values were adjusted with small volumes of 1, 0.1, 0.01, and 0.001M HCl or NaOH solutions, and closed sample vials pre-equilibrated during shaking for 12 to 24 hours. On the next day, aliquots of uranium(VI) stock solution were added to obtain the final desired total uranium(VI) concentrations. After re-adjustment of pH values, uranium(VI) sorption equilibration was allowed to take place during shaking for specified equilibration times. At specified equilibration times, final pH values were recorded and aliquots of sample suspensions were taken for analysis. For the 2-day and 21-day equilibration period, 11-mL aliquots of sample suspensions were transferred into 15-mL centrifuge vials. These sample fractions were centrifuged on a Beckman Coulter Avanti J-E (JLA 16.250 rotor at 10,000

rpm for 60 minutes), with a calculated particle-size cut-off of 43 nm, and the resulting supernatant solutions were sampled for ICP-MS and Total Inorganic Carbon (TIC) analyses.

Uranium solution concentrations were quantified by ICP-MS after acidification with TraceSelect grade HNO_3. All samples from batch sorption studies were analyzed not only for U solution concentrations, but also calcium background concentrations, as well as elements that could indicate clay dissolution or insufficient solid-liquid separations (Si, Al, Fe, etc.). For the first and last sampling time-points in the experiments with bentonite, supernatant samples were also analyzed for Total Inorganic Carbon (TIC) concentrations using a Shimadzu TOC-V Analyzer. Differences in concentrations of inorganic carbon may occur if trace carbonate minerals dissolved from the bentonite. The latter could potentially have strong influences on uranium(VI) solution speciation and sorption behavior. For 6-, 11-, and 15-day samples, only 3 mL of sample suspensions were removed and centrifuged at 10,000 rpm for 25 minutes, since no TIC analysis was performed for these samples.

For an evaluation of uranium(VI) wall sorption effects, solid phases and remaining sample solutions were discarded at the end of experiments, and vials briefly rinsed with DI-water. Sample vials were then filled with 40 mL of 2% nitric acid solutions (TraceSelect grade) in order to facilitate uranium(VI) desorption from container walls during shaking over approximately 2 weeks. Washing solutions were analyzed for concentrations of desorbed uranium(VI) as described above.

Experimental results for the batch experiments are reported in terms of distribution coefficients (K_d values) and fractions of uranium(VI) sorbed. Distribution coefficients, with units of l/kg, represent the ratio of sorbed (e.g., in mol/kg) over dissolved (e.g., in mol/l) uranium(VI) concentrations after sorption equilibration. Sorbed uranium(VI) fractions were calculated based on concentration differences between (solid-free) standards and (solid-containing) samples.

2.4   Results

Figure 2 depicts uranium(VI) sorption onto Na-montmorillonite, 'cooked' and 'uncooked' bentonite as a function of pH after a sorption equilibration of 48.5 hours (2-day samples). For both bentonite samples, the fractions of uranium(VI) sorbed are lower than for Na-montmorillonite in the circum-neutral pH region. Furthermore, the heat treatment and resulting mineral alterations in bentonite appear to further decrease uranium(VI) sorption affinities over this pH range.

Furthermore, we observed no significant time-dependent changes in uranium(VI) sorption affinities for any of the bentonite samples (Figure 3). Hence, mineral dissolution or degradation reactions with substantial effects on mineral surface characteristics and uranium(VI) solution speciation can be excluded for an experimental time-frame of 21 days.

The latter conclusion is further supported by the fact that no substantial differences were observed for Total Inorganic Carbon (TIC) concentrations between Na-montmorillonite, and 'cooked' and 'uncooked' bentonite samples after 2 days of sorption equilibration, as well as at the end of the 21-day experiments (Figure 4). Based on these TIC analysis results, a time-dependent dissolution of a large fraction of carbonate minerals in bentonite samples can be ruled out. Hence, changes in uranium(VI) solution speciation with regard to the formation of

uranium(VI)-carbonato complexes are likely not the reason for the observed changes in uranium(VI) sorption behavior.
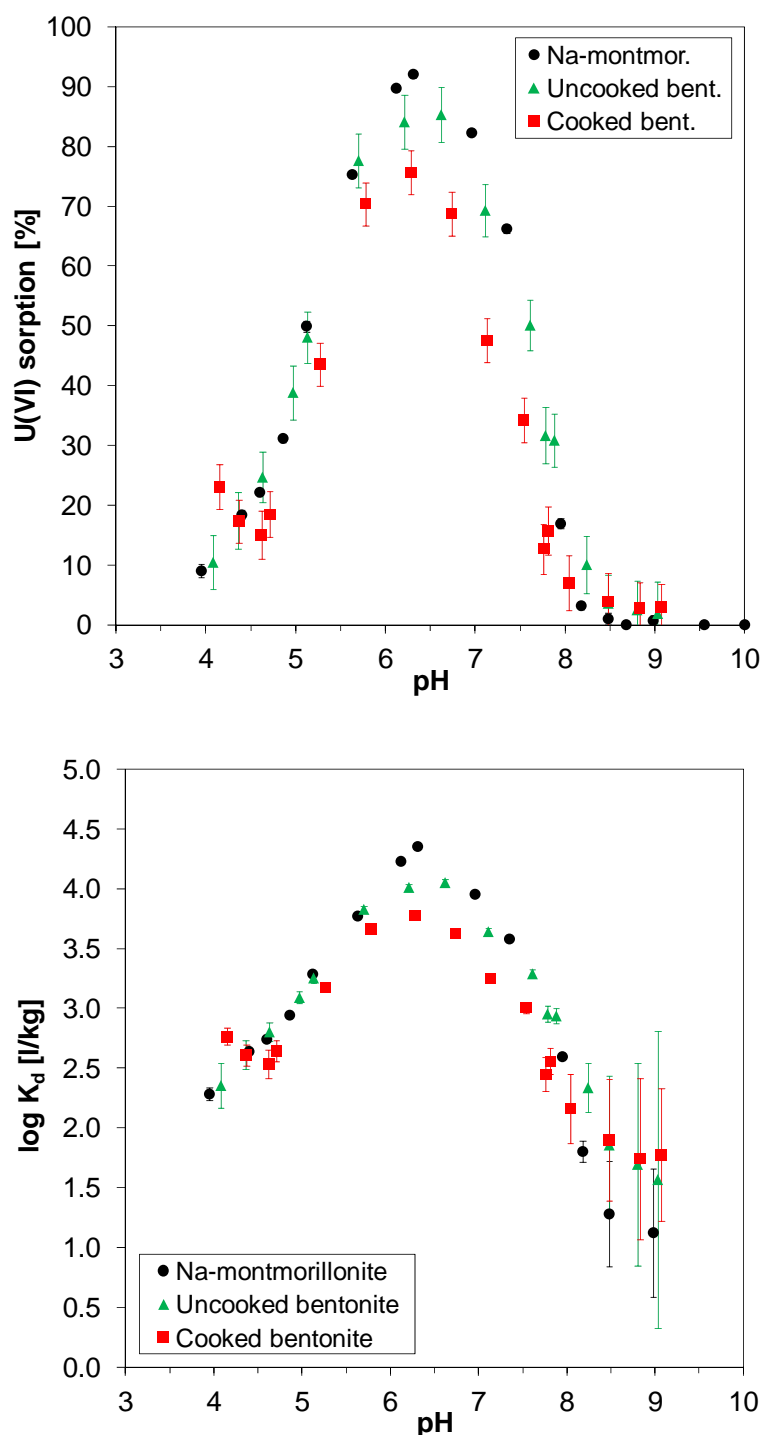
Figure 2. Uranium(VI) sorption onto 0.5 g/L sodium-montmorillonite, 'cooked' and 'uncooked' bentonite as a function of pH after sorption equilibration over 48.5 hours (2-day samples). Results are reported in terms of fractions of uranium(VI) sorbed (top) and sorption distribution coefficients (K_d values, bottom).
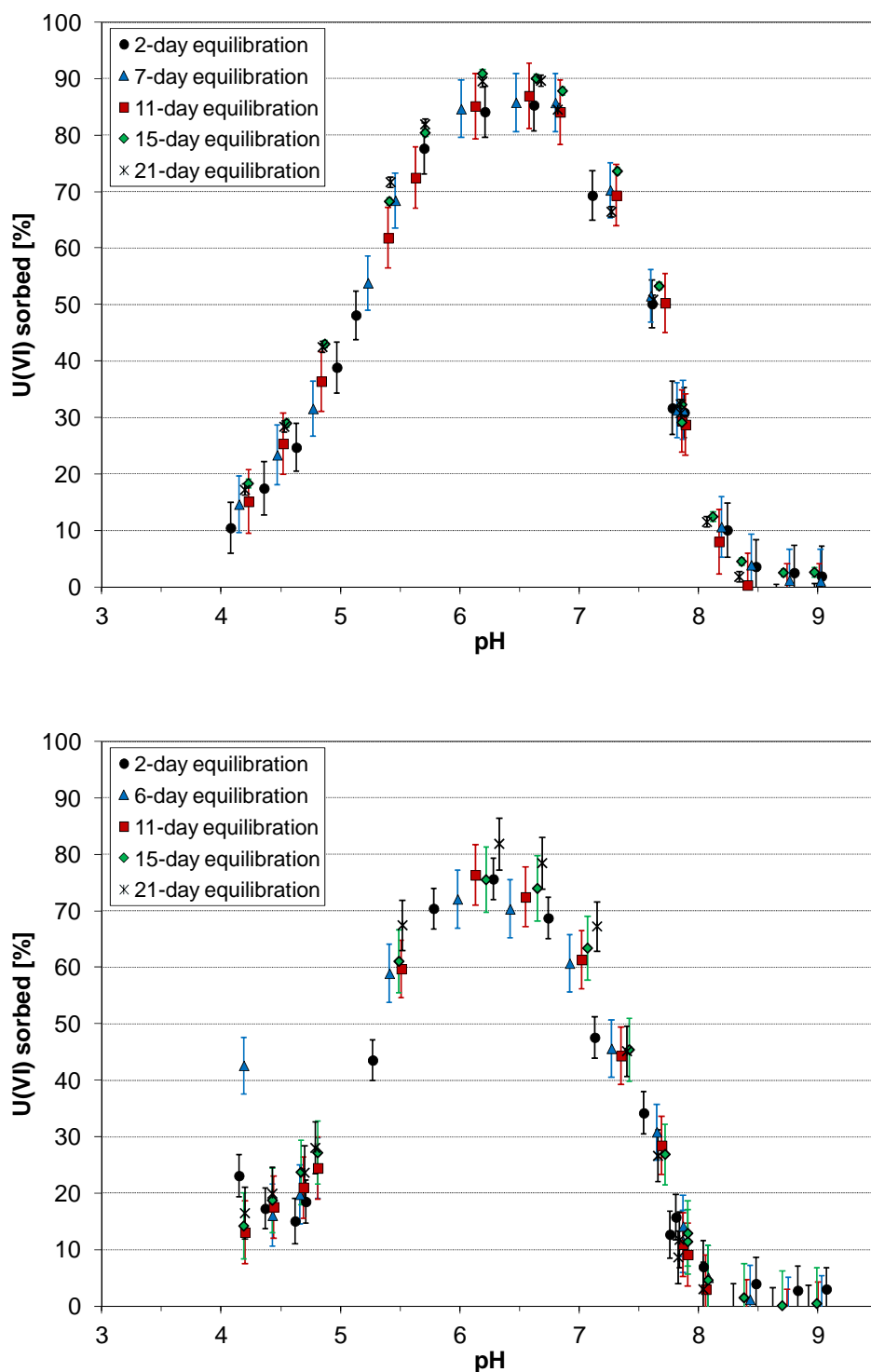
Figure 3. Time-dependent uranium(VI) sorption onto 0.5 g/L of 'cooked' and 'uncooked' bentonite samples as a function of pH and over a total sorption equilibration of 21 days. Error bars reflect analytical uncertainties for the analysis of uranium solution concentrations by ICP-MS analysis.
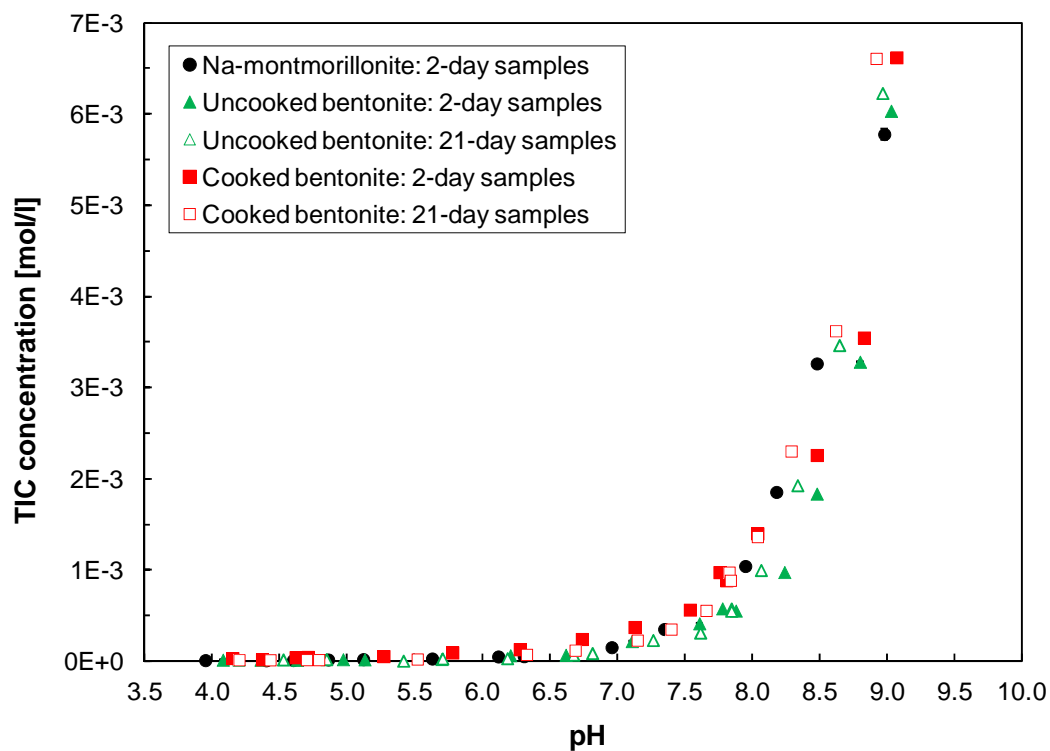
Figure 4. Comparison of Total Inorganic Carbon (TIC) concentrations in Na-montmorillonite, 'cooked' and 'uncooked' bentonite suspensions during uranium(VI) sorption experiments.

3.   DIFFUSION EXPERIMENTS

3.1   Overview and Goals

As described in detail previously (Davis et al., 2013; Rutqvist et al., 2014), our first diffusion experiment focused on the diffusive transport of calcium bromide in purified Na-montmorillonite at a low degree of compaction (dry density of 0.79 kg/l). This experiment allowed us: (1) to test our experimental approach with non-radioactive solutes prior to uranium(VI) diffusion experiments; (2) to determine diffusion coefficients for calcium (and bromide) for their later incorporation in performance assessment models, which is motivated by the strong influence of Ca on uranium(VI) solution speciation; and (3) to examine the ability of existing pore-scale conceptual models to link molecular and macroscopic scale data on adsorption and diffusion in compacted smectite. A brief summary of results for that experiment and associated modeling/simulations, and the implications of these findings for uranium(VI) diffusion in Na-montmorillonite, are provided below. Additional details can be found in a previous report (Rutqvist et al., 2014) and a companion manuscript (Tinnacher et al., in review for publication in *Geochimica et Cosmochimica Acta*).

This year, two parallel uranium(VI) diffusion experiments were begun using a very similar experimental protocol, purified Na-montmorillonite, and a comparable low degree of clay compaction. With these uranium(VI) diffusion experiments, we are pursuing the following goals: (1) to determine uranium(VI) diffusion coefficients in Na-montmorillonite (with Ca concentration levels too low to affect uranium(VI) speciation) for their later use in performance assessment models; (2) to investigate the role of full or partial anion exclusion of negatively-charged uranium(VI) solution species from montmorillonite interlayer spaces; (3) to evaluate effects of uranium(VI) sorption reactions on its diffusive transport behavior; and (4) to demonstrate an experimental approach for uranium(VI) through-diffusion experiments and provide relevant experimental data that is otherwise not accessible. We provide a summary of the currently available experimental data for the uranium(VI) diffusion experiments in Section 3.4. A detailed interpretation of the experimental results, however, which is dependent on the simulation of diffusion data after the completion of the experiment, will be reported at a later point in time.

3.2   Key Findings from Calcium Bromide Diffusion Experiment

One of the goals of this study was to examine the ability of existing pore scale conceptual models to link molecular and macroscopic scale data on adsorption and diffusion in compacted smectite. For this purpose, macroscopic scale measurements of the adsorption and diffusion of calcium, bromide, and tritiated water (HTO) in Na-montmorillonite were modeled using a multi-component reactive transport approach while testing a variety of conceptual models of pore scale properties (adsorption and diffusion in individual pores). Molecular dynamics (MD) simulations were carried out under conditions similar to those of our macroscopic scale diffusion experiments to help constrain the pore scale models.

Our evaluation of pore scale models based on experimental and modeling results suggests that *single porosity* pore scale models are consistent with results from pore scale MD simulations, but

not with macroscopic, experimental data. Among the tested conceptual models, a *dual porosity* model, which allows for a distinction between bulk liquid and diffuse ion swarm (DIS) waters, provides the best overall agreement with all results. Furthermore, our results also indicate that the pore size distribution of our compacted clay cannot be unimodal, and that Na and Ca ions adsorbed in the Stern layer retain a significant mobility. Hence, for the future development of conceptual diffusion models, an introduction of Stern layer diffusion (in addition to diffusion in bulk liquid water and DIS water) needs to be considered.

3.3   Materials and Methods for Uranium(VI) Diffusion Experiments

Uranium(VI) diffusion experiments involved a series of steps which can be summarized as follows: (1) the purification of a commercially-available Source Clay from the Clay Minerals Society (Na-montmorillonite, SWy-2) in order to minimize calcium background concentrations and quartz/feldspar impurities in the solid; (2) the purification of an in-house uranium-233 stock solution to remove accumulated daughter products and provide a known chemical solution matrix of the stock; (3) the equilibration of the purified Na-montmorillonite with background electrolyte solutions at the specified pH conditions in batch mode; (4) dry-packing of the pH-equilibration montmorillonite samples into diffusion cells followed by the saturation of the clay packings with background electrolyte solutions at the specified, target pH conditions; (5) tracer tests with tritiated water (HTO) to determine the total porosities of the clay packings in each cell; and (6) the actual uranium(VI) through-diffusion experiments.

The purification of the Na-montmorillonite Source Clay (SWy-2) has been summarized above in Section 2.2.1. In the following, we will describe the remaining experimental steps in further detail.

3.3.1   Purification of Uranium-233 Stock Solution

We selected uranium-233 as the tracer for uranium(VI) diffusion experiments due to its short half-life relative to other uranium isotopes. This allows for better detection limits of low uranium(VI) concentrations in solution, a relatively straight-forward and fast analysis by liquid scintillation counting, and hence a close and timely monitoring of diffusive fluxes over the course of diffusion experiments. As commercially available U-233 was too expensive, we utilized an existing in-house U-233 stock solution provided by Dr. Heino Nitsche (Nuclear Sciences Division, Lawrence Berkeley National Laboratory, deceased). However, a purification of this in-house stock was necessary in order to remove accumulated daughter products (Th-229, Ra-225, Ac-225), and to ensure that U-233 was present as uranium(VI) and in a known chemical solution matrix.

The purification procedure was based on the separation of uranium from impurities using an Eichrom UTEVA resin column (2-mL cartridges, 50-100 μm UTEVA resin, Eichrom P/N: UT-R50-S), while largely following the recommendations provided in Method ACW02, Rev. 1.4 (Uranium in Water) by Eichrom Technologies, LLC. During the procedure, resin columns were positioned in an Eichrom column rack (P/N AC-103) and connected to 2-mL NORM-JECT Luer sterile syringes, serving as solution reservoirs.

All acids and other chemicals used in the procedure were of TraceSelect Grade. New, acid-washed Savillex PFA vials were used to contain acids and other solutions. Furthermore, a nitric acid (3 M)-aluminum nitrate (1 M) solution was purified from known impurities of natural uranium in aluminum nitrate prior to its use in the procedure, as described in the following. A 2-mL UTEVA resin column was first conditioned with 7 mL of 3 M nitric acid in small volume increments (1 or 2 mL). Then, the nitric acid (3 M)-aluminum nitrate (1 M) solution was loaded onto the conditioned column in 2 mL increments and the purified solution, drained by gravity, collected in a fresh, clean vial.

The original U-233 stock solution (5 mL, 25 μCi total, nominal activity) was carefully dried in a Savillex PFA vial on a hot plate. The glass vial, previously containing the original stock, was rinsed with 4 mL, and then 2-times 3 mL of 5 M nitric acid. After each rinse, the individual rinse solutions were dried in the same Savillex vial. Then, U-233 was redissolved in 10 mL of 5 M nitric acid, and dried again. Finally, U-233 was dissolved in 10 mL of 3 M nitric acid-1 M aluminum nitrate solution plus 1 mL of 3.5 M $NaNO_2$. The latter was added to ensure a +6 oxidation state of U-233 in the final, purified stock.

A new 2-mL UTEVA resin column was preconditioned with 4-times 2 mL of 3 M nitric acid. Then, the solution containing U-233 was loaded onto the column in 2 mL increments, and the column effluent, which is expected to contain Ra-225, Ac-225 and possibly other impurities, collected as waste. Up to the loading of the U-233 solution, all solutions were eluted from the resin column by gravity. However, after this step, gravity-based flow-rates decreased and solutions had to be gently loaded by hand with syringes (2-mL NORM-JECT Luer sterile syringes), while ensuring sufficiently slow flow-rates (~1 mL/min.).

Next, the Savillex vial, used to dry the original U-233 stock, was rinsed with 3-times 2 mL of 3 M HNO_3, and the rinse solutions loaded onto the UTEVA column as well. This was followed by column rinses with three different types of solutions, all added in small volume increments: (1) 5 mL of 3 M HNO_3, (2) 15 mL of 8 M HNO_3, and (3) 5 mL of 9 M HCl. With the last rinse, the column resin was converted to the chloride system, and some Np and Th is expected to be removed in the process. During all of these rinses, column effluents were collected as waste. In the next step, Th-229 was removed from the column by eluting with 7-times 3 mL of 5 M HCl-0.05 M oxalic acid.

Finally, the purified U-233 was eluted from the column into three separate Savillex vials, using 5-times 2 mL of 1 M HCl (stock #1), 5-times 2 mL of 1 M HCl (stock #2), 5-times 2 mL of 0.5 M HCl (stock #3). Exact volumes of the eluted stock solutions were calculated based on weight differences before and after filling of the vials. Liquid scintillation counting (PerkinElmer Liquid Scintillation Analyzer Tri-Carb 2900TR; Ultima Gold XR liquid scintillation cocktail) of small volumes of each stock (5, 10 and 15 μL) determined specific activities of 0.61 μCi/mL (stock #1), 1.61 μCi/mL (stock #2) and 0.30 μCi/mL (stock #3) of U-233. The recovery of U-233 during the purification procedure was estimated at 100%.

3.3.2 Clay Equilibration with Desired pH-Conditions in Batch Mode

As stated above, our goal was to evaluate both, the potential influence of anion exclusion effects and uranium(VI) sorption reactions on uranium(VI) diffusion behavior in through-diffusion experiments. This required a careful selection of the experimental conditions, such as solution

pH, total uranium(VI) concentrations and degree of clay compaction, in order to ensure a breakthrough of uranium(VI) within reasonable experimental time-frames.

With regard to pH, the selected target pH conditions should ensure: (1) a predominance of anionic uranium(VI) species in solution in order to investigate potential anion exclusion effects; and (2) a sufficiently low uranium(VI) sorption affinity to montmorillonite in order to avoid strong uranium(VI) retardation that would exceed reasonable experimental time-frames. For the latter, we determined, based on preliminary calculations, that a target range of log K_d values between 0.7 and 1 [l/kg] (K_d=5-10 [l/kg]) would be appropriate. The first requirement leads to the selection of alkaline pH conditions (Figure 5). The second criterion further narrows the pH range to values between 8 and 9 (Figure 6). Hence, we decided to perform two parallel diffusion experiments at target pH values of pH-8.75 and pH-8.95, with the assumption that interactions between the clay and pH-adjusted electrolyte solutions could potentially lower the pH further, given our experience from the previous calcium bromide diffusion experiment.
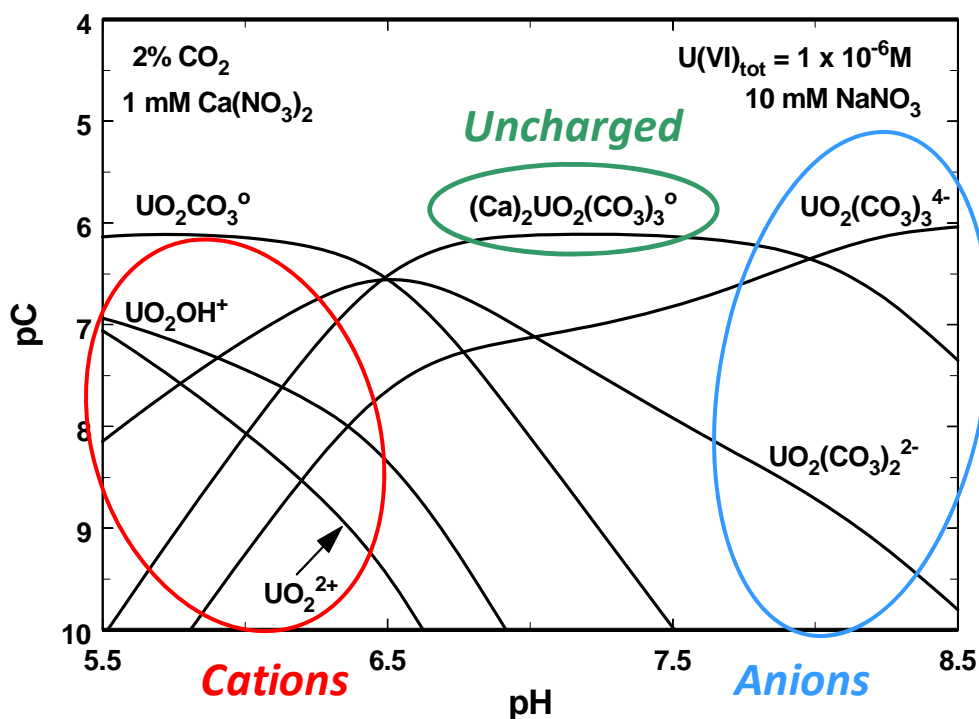

Figure 5. Distribution of cationic, anionic and neutral uranium(VI) species as a function of pH in a solution in equilibrium with a gas phase containing 2% CO_2.
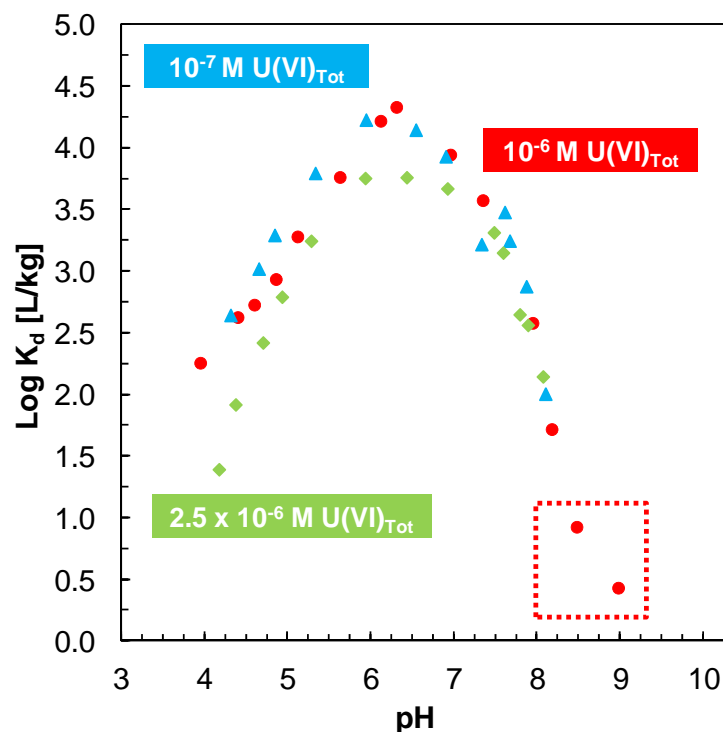
Figure 6. Results from previous uranium(VI) batch sorption experiments with Na-montmorillonite that were used to select appropriate pH conditions for uranium(VI) diffusion experiments.

The specific compositions of background electrolyte solutions at pH 8.75 and 8.95 and a total ionic strength of 0.1 M were based on aqueous speciation calculations, taking into account the ionic strength contributions of the buffer (sodium bicarbonate) and the base (sodium hydroxide) to be added for initial pH adjustments. Two-liter electrolyte solutions were prepared using high-purity chemicals (Fluka TraceSelect NaCl and NaOH; Alfa Aesar Puratronic $NaHCO_3$). After an initial equilibration of solutions with atmospheric CO_2 over two days, the pH was further adjusted by adding small volumes of high-purity HCl or NaOH.

Dry, purified Na-montmorillonite was pre-equilibrated with the background electrolyte solutions at the specified pH-conditions (pH-8.75 and pH-8.95) in batch mode in order to accelerate the equilibration process. For this purpose, six aliquots of approximately 1 gram of Na-montmorillonite were added to six acid-washed 40-mL polycarbonate centrifuge vials (Oakridge tubes). After adding 33 mL of pH-adjusted background electrolyte solutions to each vial (three vials per pH condition), the clay was first mixed by hand and then on a rotary shaker over four days. Afterwards, the pH values of the clay suspensions were recorded, and the clay separated from solutions in two consecutive centrifugations (Avanti J-E centrifuge, JA-17 rotor, 16,000 rpm for 33 minutes each). After re-combining all clay fractions in the original polycarbonate vials, 20 mL of fresh background electrolyte solutions were added to each individual vial, and the clay mixing and equilibration steps repeated.

This series of steps was repeated further for a total number of 10 equilibration steps over three weeks (individual equilibration times of 4, 0.8, 0.8, 1, 3.8, 0.9, 1, 0.9, 2.9, and 1 days). (Over this

time-frame, the pH values in electrolyte solutions not in contact with clay remained stable.) Afterwards, three pH fine-adjustments were performed by adding small volumes of HCl and NaOH solutions directly to the individual vials over three days, while allowing for system equilibration over about one day after each adjustment. An overview of the changing pH conditions after each equilibration or adjustment step is provided in Figure 7.
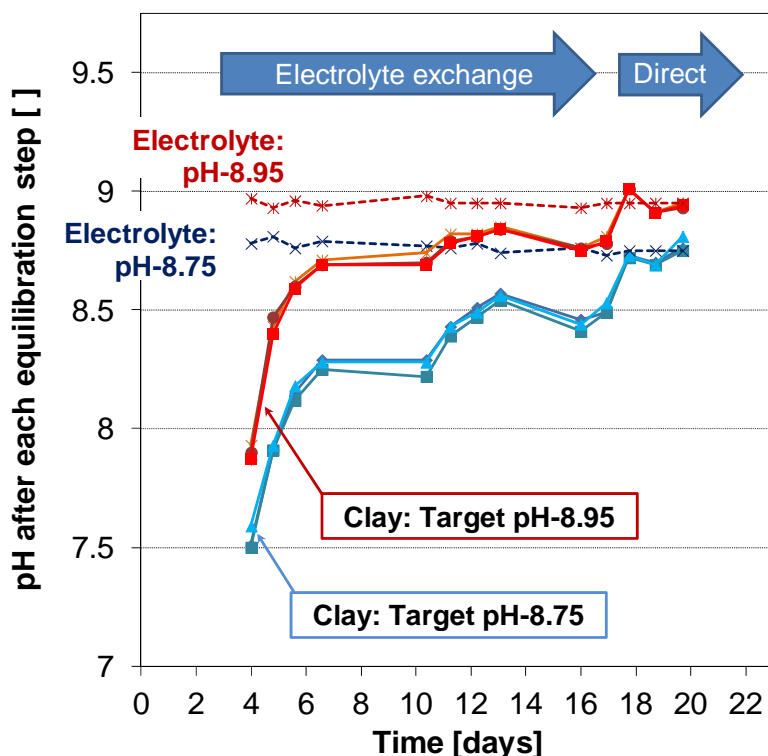
Figure 7. Overview of pH-equilibration of Na-montmorillonite in preparation for uranium(VI) diffusion experiments. Blue arrows indicate changes in the equilibration procedure from the exchange of background electrolyte solutions to a direct pH adjustment with HCl and NaOH solutions.

Once the pH conditions in the suspensions appeared to remain stable, the clay samples were isolated from solutions by centrifugation as described above, and dried in a convection oven at 45 °C over five days. After grinding of the dry clay samples in a Retsch MM 400 ball mill (frequency of 30/sec for 2 minutes), the pH-equilibrated samples were ready for their use in later uranium(VI) diffusion experiments.

3.3.3 Experimental Setup for Uranium(VI) Diffusion Experiments

The uranium(VI) through-diffusion experiments largely followed procedures previously described in the literature (Molera and Eriksen, 2002; Van Loon et al., 2003a;b). The experimental setup consists of a set of two diffusion cells, each connected to high- and low-concentration reservoirs, and a peristaltic pump (**Error! Reference source not found.** 8). All experimental solutions were repeatedly adjusted to the target pH values of pH 8.75 and 8.95

using small volumes of acid/base solutions (TraceSelect grade NaOH and HCl) while equilibrating with atmospheric CO_2, prior to their contact with the mineral phase.
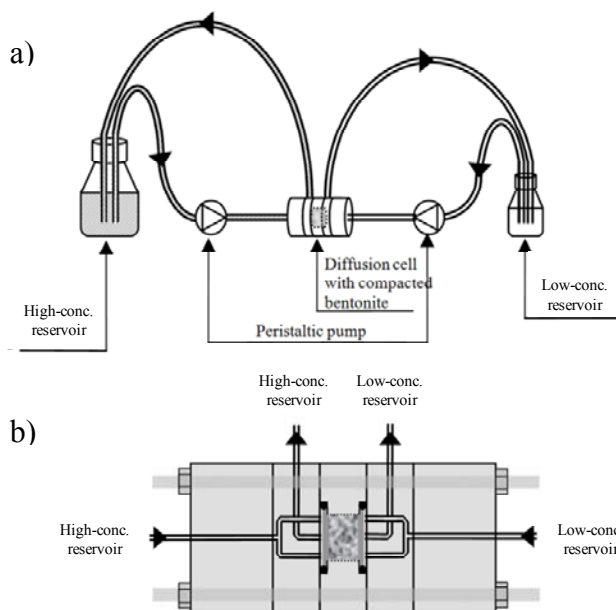

Figure 8. Schematic of the experimental apparatus for uranium(VI) diffusion studies.

At the beginning of the experiment, dry, pH-adjusted Na-montmorillonite samples were packed into the diffusion cells (PEEK; D=1.0 cm, L=0.5 cm; Alltech 2 μm stainless-steel frits, P/N 721825) by hand with the goal to obtain a dry bulk density of approximately 0.8 kg dm^{-3}. The clay was carefully compacted with a custom-made PEEK rod, and then saturated with the individual background electrolyte solutions (0.1 M NaCl, pH-8.75 or pH-8.95) by circulating electrolyte solutions for about 3 ½ weeks (two 200-mL reservoirs per cell; estimated flow rate of 0.78 mL min^{-1}). The exact dry densities of the clay packings (0.77 kg dm^{-3} for both cells) were calculated after determining the water content of the clay samples based on drying at 150 °C for approximately five days.

After clay saturation, tracer tests with tritiated water (HTO) were initiated by replacing the reservoir solutions with 200 mL of background electrolytes at pH-8.75 or pH-8.95 containing ~24 nCi/mL (~890 Bq mL^{-1}) HTO (high-concentration reservoirs) on one end of each diffusion cell, and 20 mL reservoirs containing fresh, HTO-free electrolyte solutions (low-concentration reservoirs) on the opposite ends. Over the following weeks, the circulation of solutions was continued at the same flow rate. Electrolyte solutions in the low-concentration reservoirs were repeatedly replaced in order to maintain a nearly constant concentration gradient between the high- and low-concentration reservoirs. The exchanged low-concentration reservoir vials were weighed to correct for volume losses due to evaporation. Solutions were sampled for tritium analysis by liquid scintillation counting (PerkinElmer Liquid Scintillation Analyzer Tri-Carb 2900TR; Ultima Gold XR liquid scintillation cocktail), and their solution pH values were

recorded. This procedure was continued until a series of data points had been collected under steady-state conditions for HTO diffusive fluxes.

The solutions in the high-concentration reservoirs were then replaced with HTO-free background electrolyte solutions at pH-8.75 and pH-8.95 containing a nominal concentration of 2.5×10^{-6} M uranium(VI) in the form of the U-233 tracer (exact concentrations were 2.36×10^{-6} M U-233 or 5.35 nCi/mL = 198 Bq/mL for pH-8.75, and 2.34×10^{-6} M U-233 or 5.30 nCi/mL = 196 Bq/mL for pH-8.95). Again, low-concentration reservoir solutions were continuously replaced, and uranium-233 and tritium activities analyzed (PerkinElmer Liquid Scintillation Analyzer Tri-Carb 2900TR; Ultima Gold XR liquid scintillation cocktail), with the goal to collect a sufficient number of data points under steady-state conditions for uranium(VI) diffusive fluxes in each system. In addition, the pH values in low-concentration reservoir solutions were measured. Furthermore, samples from low-concentration reservoir solutions were preserved for a later ICP-MS analysis of a series of elements that could either be relevant for uranium(VI) solution speciation or indicate any potential montmorillonite degradation, as wells as for alkalinity titrations (both analyses currently in progress).

It is important to note that, with the replacement of HTO high-concentration reservoir solutions with U-233 high-concentration reservoir solutions, we essentially started an 'out-diffusion' experiment for tritium. At the end of the tritium tracer test, and after reaching steady-state conditions, a linear HTO concentration profile had been established across the clay packing in the diffusion cell. By replacing the high-concentration reservoir with a HTO-free solution and continuously exchanging low-concentration reservoir solutions during the uranium(VI) diffusion experiments, new concentration gradients between HTO in the diffusion cells and the reservoir solutions are established. Hence, HTO diffuses out of the cells in both directions, and is accumulated in both the high- and low-concentration reservoir solutions. As a result, low HTO concentrations are detected in low-concentration reservoir solutions during the uranium(VI) diffusion experiments. These 'out-diffusion' data for HTO will allow us to further constrain total porosity values that are inferred from simulations of HTO through-diffusion data.

Last, given the high importance of pH for uranium(VI) solution speciation and sorption behavior, we performed two additional pH measurements at two other points in the experimental setup during uranium(VI) diffusion, besides the values collected for low-concentration reservoir solutions. First, a small pH probe was directly immersed into the two high-concentration reservoir solutions containing U-233 over the course of the experiment. In addition, we collected small volumes (3-5 mL) of 'flow-back' solutions, which are high-concentration reservoir solutions that had been in contact with the clay packings in the diffusion cells and were flowing back into the high-concentration reservoirs. After these pH measurements, collected solution fractions were returned to their respective reservoirs. These additional measurements were taken in order to check whether the pH values directly recorded in high-concentration reservoir solutions actually represented the conditions of solutions in contact with the clay packings. This consideration is based on the large dilution effects occurring in high-concentration reservoirs during the circulations of solutions (200 mL of reservoir volume versus 0.78 mL min^{-1} flow-rate for the circulating solution). However, both of these types of measurements were performed much less frequently in order to minimize any potential disturbances to the experiments.

3.4   Results

3.4.1   pH Monitoring Data for Uranium(VI) Diffusion Experiments

In Figure 9, we provide a summary of pH monitoring data recorded during the HTO tracer tests and over the course of the (ongoing) uranium(VI) diffusion experiments. It appears that the contact of background electrolyte solutions with the clay packings causes a slight drop in pH in both systems. However, other than this initial pH drop, the pH conditions are reasonably stable over time and across the individual diffusion cells in both systems. Hence, the pH pre-equilibration step in batch mode allowed for a reasonable stabilization of pH conditions in later diffusion experiments. The latter will simplify the simulation and interpretation of diffusion data, given the strong dependence of uranium(VI) solution speciation and sorption behavior on pH.
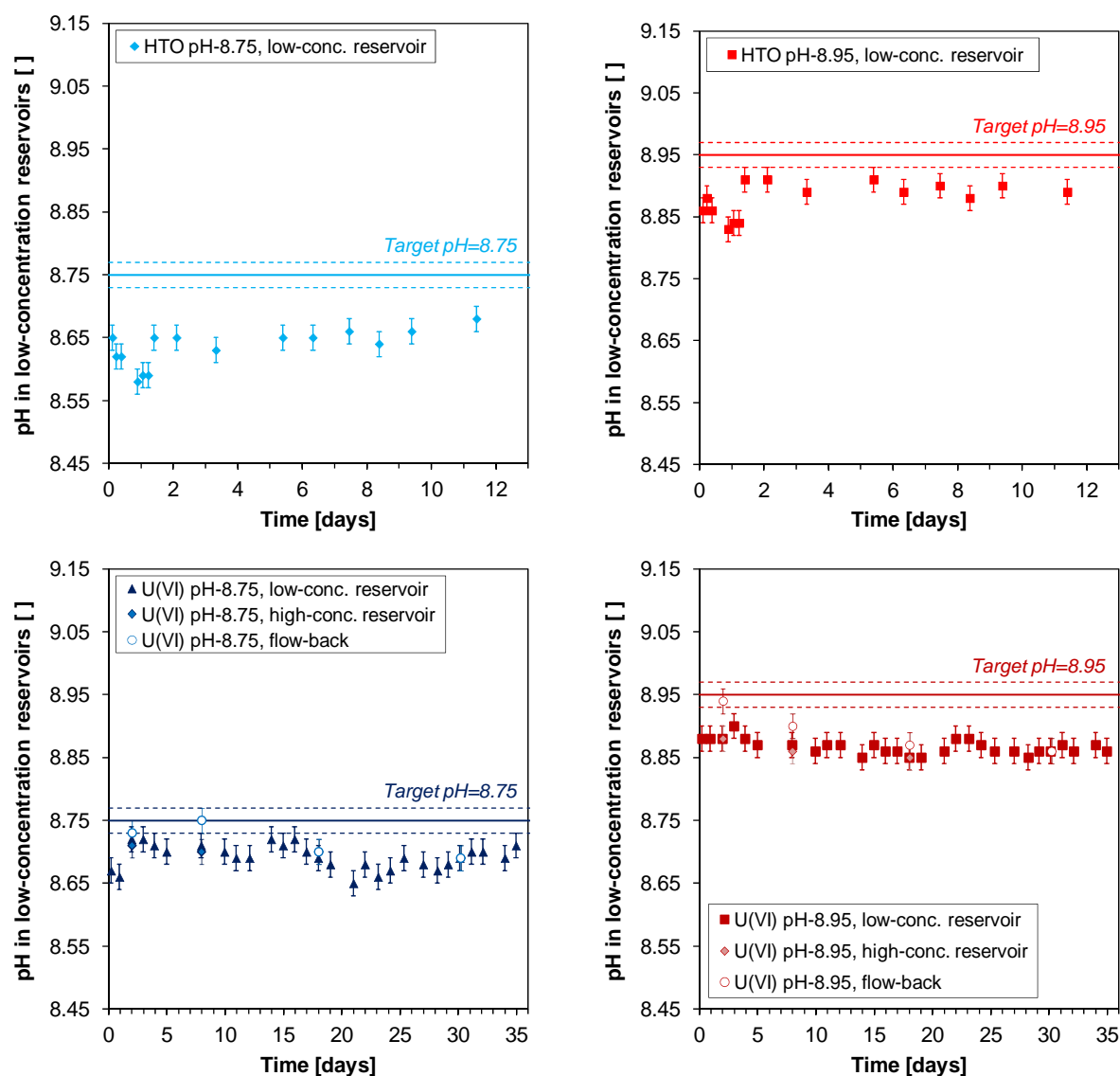

Figure 9. pH monitoring data for HTO tracer test and uranium(VI) diffusion experiments.

The pH values in 'flow-back' solutions appear to be slightly higher and closer to target pH values than in high-concentration reservoir solution at early time-points in the experiment. However, otherwise no apparent trends regarding pH differences between high-concentration reservoir solutions and flow-back solutions were observed.

3.4.2 Results for Tritium Tracer Tests

Normalized mass flux densities reaching the low-concentration reservoir (J_N in m day^{-1}) were calculated with the following expression:

$$J_N = \frac{C_{low}}{C_{high}} \frac{V_{low}}{A \Delta t}$$

1

where C_{low} is the concentration of the species of interest measured in the low-concentration reservoir at a sampling event, C_{high} is the constant concentration in the high-concentration reservoir, Δt is the time interval since the previous sampling event (in days), A is the cross sectional area available for diffusion (0.785 cm^2), and V_{low} is the volume of the low-concentration reservoir (about 20 mL). (With the exchange of low-concentration reservoir solutions, C_{low} is initially zero at the beginning of each individual time interval.)

Figure 10 depicts the results for normalized HTO fluxes recorded during the HTO tracer tests (HTO through-diffusion data) and the (ongoing) uranium(VI) diffusion experiments (HTO out-diffusion data), respectively. Based on the results for HTO through-diffusion (Figure 10, top), we can conclude that the total porosity of the clay packing in the pH-8.75 system is slightly higher than for the pH-8.95 system. This agrees well with our estimated dry density values for the two cells, with 0.766 and 0.772 kg dm^{-3} for pH-8.75 and pH-8.95 systems, respectively. Slightly higher dry densities and degrees of clay compaction would result in slightly lower total porosities of the clay packing. A later simulation of both types of experimental data sets will allows us to determine the total porosity and water diffusion coefficients in each system.

3.4.3 Results for Uranium(VI) Through-Diffusion

Based on currently available data, observed normalized fluxes for uranium(VI) are about one order of magnitude lower than fluxes for tritiated water (Figure 11). Furthermore, under both pH conditions, uranium(VI) breakthrough is retarded relative to the non-reactive tracer tritium, with a greater retardation at target pH-8.75 than pH-8.95. The latter is in good agreement with uranium(VI) sorption data, which indicate higher uranium(VI) sorption affinities and K_d values at pH-8.75 than pH-8.95.

Given that the currently observed uranium(VI) fluxes are substantially lower than for HTO, we assume at this point that this will also be the case under steady-state conditions for uranium(VI) fluxes. Hence, a significant contribution of uranium(VI) surface diffusion to the total fluxes, and a strong influence of weak uranium(VI) sorption reactions, e.g. in the form of cation exchange reactions, can most likely be ruled out for these systems. Last, there seems to be a stronger kinetic component for uranium(VI) sorption reactions at pH-8.75 than at pH-8.95 (Figure 12), since the time-frames required to reach steady-state conditions appear to be different for these two systems. This indicates a potential overall rate dependence on the aqueous speciation of

uranium(VI), perhaps related to the dissociation kinetics of different aqueous uranium(VI) complexes prior to the formation of uranium(VI) surface complexes at montmorillonite edge sites.
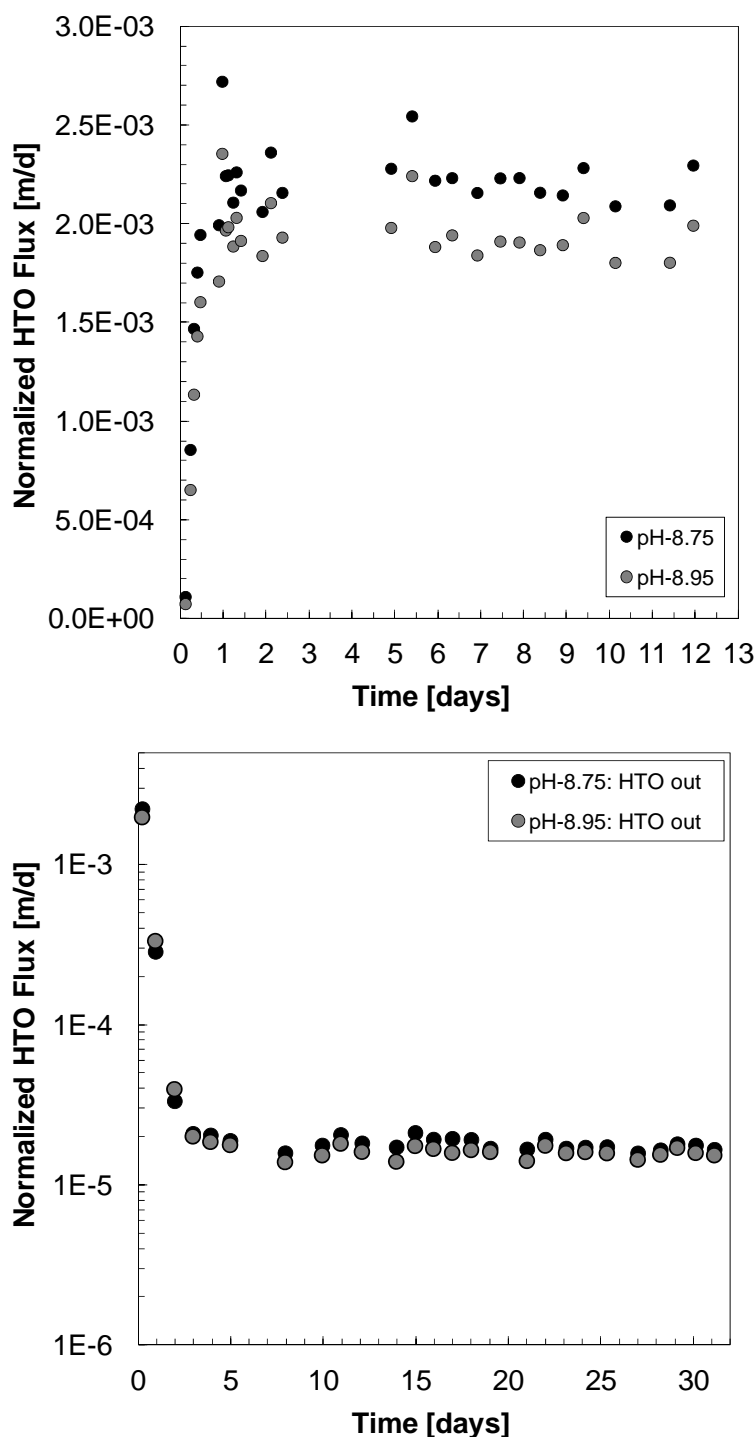
Figure 10. Normalized HTO diffusive fluxes in low-concentration reservoirs during HTO tracer tests (HTO through-diffusion experiments, top) and uranium(VI) through-diffusion experiments (HTO out-diffusion experiments, bottom) at target pH values of 8.75 and 8.95.
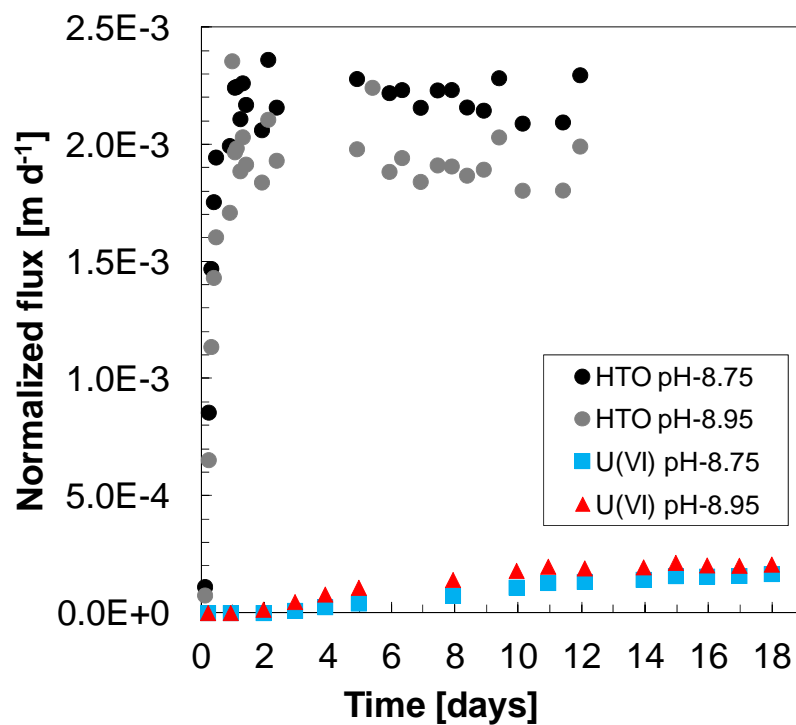
Figure 11. Comparison of normalized diffusive fluxes for tritiated water (HTO) and uranium(VI) at target pH values of 8.75 and 8.95.

Figure 12. Normalized uranium(VI) diffusive fluxes during uranium(VI) through-diffusion experiments at target pH values of 8.75 and 8.95.

4. FUTURE WORK

The following tasks are planned for the upcoming year:

1) Continue data collection and analysis for the ongoing uranium(VI) diffusion experiment in purified Na-montmorillonite until a sufficient number of data points has been collected under steady-state conditions for diffusive uranium(VI) fluxes at both pH conditions.

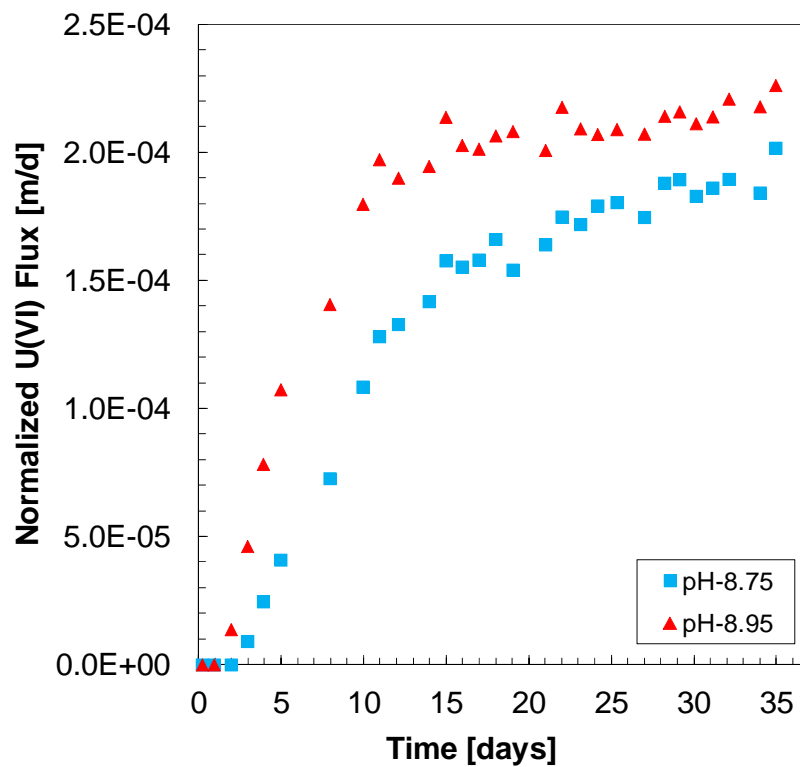2) Simulation of the uranium(VI) diffusion data in collaboration with modelers, with the goal to elucidate the following research questions: (a) the potential influence of anion exclusion effects, and (b) the relevance of uranium(VI) cation exchange versus surface complexation reactions for the diffusive transport behavior of uranium(VI) under alkaline conditions.

An evaluation of these questions is needed in order to develop realistic conceptual models for diffusion process models in conjunction with performance assessment models. In addition, the determination of uranium(VI) diffusion coefficients, resulting from the simulations of these data sets, will directly provide input parameters for later performance models. The latter, however, requires that future performance assessment models are capable of tracking changes in aqueous compositions over time and space.

While the data from the current uranium(VI) – Na-montmorillonite diffusion experiments at alkaline pH conditions will represent an important step towards the development of a realistic, conceptual uranium(VI)-diffusion model, we are also proposing a new set of parallel diffusion experiments in Na-montmorillonite. These experiments will be performed under acidic pH conditions, with pH values specifically selected to show similar uranium(VI) sorption distribution coefficients (K_d values) as in the current experiments under alkaline pH. At low pH, uranium(VI) is primarily present in the form of cationic solution species, which are expected to sorb onto montmorillonite in the form of (weak) cation exchange reactions. Hence, given our current understanding of these systems, this should result in comparable uranium(VI) retardation, as observed under alkaline conditions, but significantly higher diffusive fluxes of uranium(VI). Experimental evidence supporting this hypothesis is strongly needed in order to allow for a realistic prediction of uranium(VI) mobility at a range of pH conditions.

Furthermore, additional uranium(VI) diffusion experiments are planned for different types of solids, namely 'cooked' and 'uncooked' bentonite samples. Current data describing uranium(VI) sorption behavior to these solids suggest a decrease in uranium(VI) sorption after the exposure of bentonite to heat, which may also affect uranium(VI) retardation during diffusion in these systems. Prior to performing this new set of diffusion experiments, we will characterize uranium(VI) sorption behavior to a series of other heat-treated bentonite/clay samples. For instance, uranium(VI) sorption experiments with bentonite samples from the FEBEX heater test will allow us to evaluate if a substantially longer exposure to heat (over years versus weeks), but at a lower temperature (100 °C versus 300 °C), increases or decreases the observed temperature effects on uranium(VI) sorption behavior. Furthermore, we will use heat-treated Opalinus Clay samples for additional comparisons. Typically, Opalinus Clay contains small fractions of pyrite, which are known to lead to a surface reduction of uranium(VI) to uranium(IV), at least under anaerobic conditions (e.g., Bruggeman and Maes, 2010), potentially resulting in a higher apparent fraction of uranium sorbed. Our goal is to investigate whether a potential decrease in the pyrite fraction due to heat-treatment could cause a change in uranium sorption characteristics. We will collaborate with Dr. Liange Zheng (LBNL) and Dr. Florie Caporuscio at Los Alamos National Laboratory in order to obtain these bentonite and clay samples.

Given the time-consuming nature of diffusion experiments, the results from this series of uranium(VI) sorption experiments will allow us to select a solid phase that is expected to cause the biggest differences in uranium(VI) diffusion behavior relative to Na-montmorillonite, as well as the appropriate system conditions for these experiments.

With regard to publications, we expect to complete the surface complexation modeling of the uranium(VI) – Na-montmorillonite systems and submit a related manuscript within the next fiscal year. In addition, we will work toward a publication describing the uranium(VI) diffusion data and modeling results for the Na-montmorillonite system.

5. ACKNOWLEDGMENT

6. REFERENCES

Altmann, S., 2008. 'Geo'chemical research: A key building block for nuclear waste disposal safety cases. *J. Contam. Hydrol.* 102, 174–179.

Altmann, S., Tournassat, C., Goutelard, F., Parneix, J.-C., Gimmi, T., Maes, N., 2012. Diffusion-driven transport in clayrock formations. *Appl. Geochem.* 27, 463–478.

ANDRA, 2005. Référentiel du comportement des radionucléides et des toxiques chimiques d'un stockage dans le Callovo-Oxfordien jusqu'à l'Homme. (No. Dossier 2005 Argile). Dossier 2005 Argile. Agence Nationale pour la gestion des déchets radioactifs, Châtenay-Malabry, France.

Appelo, C.A.J., Van Loon, L.R., Wersin, P., 2010. Multicomponent diffusion of a suite of tracers (HTO, Cl, Br, I, Na, Sr, Cs) in a single sample of Opalinus Clay. *Geochim. Cosmochim. Acta* 74, 1201–1219.

Appelo, C.A.J., Wersin, P., 2007. Multicomponent diffusion modeling in clay systems with application to the diffusion of tritium, iodide, and sodium in Opalinus clay. *Env. Sci. Tech.* 41, 5002–5007.

Bai, J., C. X. Liu and W. P. Ball 2009. Study of Sorption-Retarded U(VI) Diffusion in Hanford Silt/Clay Material. Environmental Science & Technology 43 (20): 7706-7711.

Bock, H., Dehandschutter, B., Martin, C.D., Mazurek, M., De Haller, A., Skoczylas, F., Davy, C., 2010. Self-sealing fractures in argillaceous formations in the context of geological disposal of radioactive was (No. 6184). Nuclear energy agency, organisation for economic co-operation and development.

Bradbury, M.H., Baeyens, B., 2011. Predictive sorption modelling of Ni(II), Co(II), Eu(IIII), Th(IV) and U(VI) on MX-80 bentonite and Opalinus Clay: A "bottom-up" approach. *Appl. Clay Sci.* 52, 27–33.

Brown, P.L., Haworth, A., Sharland, S.M., Tweed, C.J. 1991. Modelling studies of the sorption of radionuclides in the far field of nuclear waste repository. *Radiochim. Acta*, 52/53, 439-443.

Bruggeman, C., Maes, N., 2010. Uptake of uranium(VI) by pyrite under Boom Clay conditions: Influence of dissolved organic carbon. *Environ. Sci. Technol.*, 44, 4210-4216.

Caporuscio, F.A., Cheshire, M.C., Rearick, M.S., McCarney, M.K., Jove-Colon, C. 2013. EBS Report - LANL Experimental update of buffer/backfill at elevated P,T. DOE Report number: FCRD-UFD-2013-000207.

Caporuscio, F.A., Cheshire, M.C., Rearick, M.S., Jove-Colon, C. 2014. LANL Argillite EBS Experimental Program 2014. FCRD-UFD-2014-000491.

Cheshire, M.C., Caporuscio, F.A., Rearick, M.S., Jove-Colon, C., McCarney, M.K. 2014. Bentonite evolution at elevated pressures and temperatures: An experimental study for generic nuclear repository designs. *American Mineralogist*, 99, 1662-1675.

Choi, J.-W., Oscarson, D., 1996. Diffusive transport through compacted Na-and Ca-bentonite. *J. Contam. Hydrol.* 22, 189–202.

Davis, J., Rutqvist, J., Steefel, C., Tinnacher, R., Vilarrasa, V., Zheng, L., Bourg, I., Liu H.-H., Birkholzer, J. Investigation of Reactive Transport and Coupled THM Processes in EBS:

FY13 Report, Lawrence Berkeley National Laboratory, DOE Used Fuel Disposition Campaign, FCRD-UFD-2013-000216. (2013).

Delay, J., Vinsot, A., Krieguer, J.-M., Rebours, H., Armand, G., 2007. Making of the underground scientific experimental programme at the Meuse/Haute-Marne underground research laboratory, North Eastern France. *Phys. Chem. Earth, Parts A/B/C* 32, 2–18.

Descostes, M., Blin, V., Bazer-Bachi, F., Meier, P., Grenut, B., Radwan, J., Schlegel, M.L., Buschaert, S., Coelho, D., Tevissen, E., 2008. Diffusion of anionic species in Callovo-Oxfordian argillites and Oxfordian limestones (Meuse/Haute-Marne, France). *Appl. Geochem.* 23, 655–677.

Englert, M., Krall, L., Ewing, R.C., 2012. Is nuclear fission a sustainable source of energy? *MRS bulletin* 37, 417–424.

García-Gutiérrez, M., J. L. Cormenzana, T. Missana, M. Mingarro and U. Alonso 2003. Analysis of uranium diffusion coefficients in compacted FEBEX bentonite. Scientific Basis for Nuclear Waste Management XXVII, Kalmar, Sweden, Materials Research Society.

García-Gutiérrez, M., Cormenzana, J.L., Missana, T., Mingarro, M., 2004. Diffusion coefficients and accessible porosity for HTO and ^{36}Cl in compacted FEBEX bentonite. *Appl. Clay Sci.* 26, 65–73.

Gimmi, T., Kosakowski, G., 2011. How mobile are sorbed cations in clays and clay rocks? *Env. Sci. Tech.* 45, 1443–1449.

Glaus, M., Baeyens, B., Bradbury, M.H., Jakob, A., Van Loon, L.R., Yaroshchuk, A., 2007. Diffusion of ^{22}Na and ^{85}Sr in montmorillonite: evidence of interlayer diffusion being the dominant pathway at high compaction. *Environ. Sci. Technol.* 41, 478–485.

Glaus, M.A., Birgersson, M., Karnland, O., Van Loon, L.R., 2013. Seeming steady-state uphill diffusion of ^{22}Na$^+$ in compacted montmorillonite. *Env. Sci. Tech.* 47, 11522–11527.

Glaus, M.A., Frick, S., Rosse, R., Van Loon, L.R., 2010. Comparative study of tracer diffusion of HTO, Na-22(+) and Cl-36(-) in compacted kaolinite, illite and montmorillonite. *Geochim. Cosmochim. Acta* 74, 1999–2010.

Glaus, M.A., Frick, S., Rossé, R., Van Loon, L.R., 2011. Consistent interpretation of the results of through-, out-diffusion and tracer profile analysis for trace anion diffusion in compacted montmorillonite. *J. Contam. Hydrol.* 123, 1–10.

Glaus, M.A., Müller, W., Van Loon, L.R., 2008. Diffusion of iodide and iodate through Opalinus Clay: Monitoring of the redox state using an anion chromatographic technique. *Appl. Geochem.* 23, 3612–3619.

Gonzàlez Sànchez, F., Van Loon, L.R., Gimmi, T., Jakob, A., Glaus, M.A., Diamond, L.W., 2008. Self-diffusion of water and its dependence on temperature and ionic strength in highly compacted montmorillonite, illite and kaolinite. *Appl. Geochem.* 23, 3840–3851.

Guyonnet, D., Touze-Foltz, N., Norotte, V., Pothier, C., Didier, G., Gailhanou, H., Blanc, P., Warmont, F., 2009. Performance-based indicators for controlling geosynthetic clay liners in landfill applications. *Geotext. Geomembranes* 27, 321–331.

Holmboe, M., Karin Norrfors, K., Jonsson, M., Wold, S., 2011. Effect of textgreekg-radiation on radionuclide retention in compacted bentonite. *Radiat. Phys. Chem.* 80, 1371–1377.

Horseman, S.T., Volckaert, G., 1996. Disposal of radioactive wastes in argillaceous formations. *Geological Society, London, Engineering Geology Special Publications* 11, 179–191.

IAEA, 2004. Implications of partitioning and transmutation in radioactive waste management, *Technical reports series*. International Atomic Energy Agency, Vienna.

Jakob, A., Pfingsten, W., Van Loon, L.R., 2009. Effects of sorption competition on caesium diffusion through compacted argillaceous rock. *Geochim. Cosmochim. Acta* 73, 2441–2456.

Jansson, M., Eriksen, T.E., 2004. In situ anion diffusion experiments using radiotracers. *J. Contam. Hydrol.* 68, 183–192.

Jenny, H., Overstreet, R., 1939. Surface Migration of Ions and Contact Exchange. *J. Phys. Chem.* 43, 1185–1196.

Joseph, C., Schmeide, K., Sachs, S., Brendler, V., Geipel, G., Bernhard, G., 2011. Sorption of uranium (VI) onto Opalinus Clay in the absence and presence of humic acid in Opalinus Clay pore water. *Chem. Geol.* 284, 240–250.

Joseph, C., Van Loon, L.R., Jakob, A., Steudtner, R., Schmeide, K., Sachs, S., Berhard, G. 2013. Diffusion of U(VI) in Opalinus Clay: influence of temperature and humic acid. *Geochim. Cosmochim. Acta*, 109, 74-89.

Jougnot, D., Revil, A., Leroy, P., 2009. Diffusion of ionic tracers in the Callovo-Oxfordian clay-rock using the Donnan equilibrium model and the formation factor. *Geochim. Cosmochim. Acta* 73, 2712–2726.

Kaszuba, J.P., Runde, W.H., 1999. The aqueous geochemistry of neptunium: Dynamic control of soluble concentrations with applications to nuclear waste disposal. *Env. Sci. Tech.* 33, 4427–4433.

Kerisit, S., Liu, C., 2010. Molecular simulation of the diffusion of uranyl carbonate species in aqueous solution. *Geochim. Cosmochim. Acta* 74, 4937–4952.

Korichi, S., A. Bensmaili and M. Keddam 2010. Reactive Diffusion of Uranium in Compacted Clay: Evaluation of Diffusion Coefficients by a Kinetic Approach. Defect and Diffusion Forum 297-301: 275-280.

Kozaki, T., Fujishima, A., Saito, N., Sato, S., Ohashi, H., 2005. Effects of dry density and exchangeable cations on the diffusion process of sodium ions in compacted montmorillonite. *Eng. Geol.* 81, 246–254.

Kozaki, T., Fujishima, A., Sato, S., Ohashi, H., 1998a. Self-diffusion of sodium ions in compacted montmorillonite. *Nucl. Technol.* 121, 63–69.

Kozaki, T., Inada, K., Sato, S., Ohashi, H., 2001. Diffusion mechanism of chloride ions in sodium montmorillonite. *J. Contam. Hydrol.* 47, 159–170.

Kozaki, T., Liu, J.H., Sato, S., 2008. Diffusion mechanism of sodium ions in compacted montmorillonite under different NaCl concentration. *Phys. Chem. Earth, Parts A/B/C* 33, 957–961.

Kozaki, T., Saito, N., Fujishima, A., Sato, S., Ohashi, H., 1998b. Activation energy for diffusion of chloride ions in compacted sodium montmorillonite. *J. Contam. Hydrol.* 35, 67–75.

Kozaki, T., Sato, H., Fujishima, A., Saito, N., Sato, S., Ohashi, H., 1996. Effect of dry density on activation energy for diffusion of strontium in compacted sodium montmorillonite. In: *MRS Proceedings*. Cambridge Univ Press, p. 893.

Kozaki, T., Sato, H., Sato, S., Ohashi, H., 1999a. Diffusion mechanism of cesium ions in compacted montmorillonite. *Eng. Geol.* 54, 223–230.

Kozaki, T., Sato, Y., Nakajima, M., Kato, H., Sato, S., Ohashi, H., 1999b. Effect of particle size on the diffusion behavior of some radionuclides in compacted bentonite. *J. Nucl. Mater.* 270, 265–272.

Kozaki, T., Sawaguchi, T., Fujishima, A., Sato, S., 2010. Effect of exchangeable cations on apparent diffusion of Ca^{2+} ions in Na-and Ca-montmorillonite mixtures. *Phys. Chem. Earth, Parts A/B/C* 35, 254–258.

Lee, J.O., Cho, W.J., Hahn, P.S., Lee, K.J., 1996. Effect of dry density on Sr-90 diffusion in a compacted Ca-bentonite for a backfill of radioactive waste repository. *Ann. Nucl. Energy* 23, 727–738.

Loomer, D.B., Scott, L., Al, T.A., Mayer, K.U., Bea, S., 2013. Diffusion–reaction studies in low permeability shale using X-ray radiography with cesium. *Appl. Geochem.* 39, 49–58.

Liu, C., L. Zhong and J. M. Zachara 2010. Uranium(VI) diffusion in low-permeability subsurface materials. Radiochimica Acta 98 (9-11): 719-726.

Maes, N., H. Moors, L. Wang, G. Delecaut, P. De Canniere and M. Put 2002. The use of electromigration as a qualitative technique to study the migration behaviour and speciation of uranium in the Boom Clay. Radiochimica Acta 90 (9-11): 741-746.

Mazurek, M., Alt-Epping, P., Bath, A., Gimmi, T., Niklaus Waber, H., Buschaert, S., Cannière, P.D., De Craen, M., Gautschi, A., Savoye, S., Vinsot, A., Wemaere, I., Wouters, L., 2011. Natural tracer profiles across argillaceous formations. *Appl. Geochem.* 26, 1035–1064.

Melkior, T., Gaucher, E.C., Brouard, C., Yahiaoui, S., Thoby, D., Clinard, C., Ferrage, E., Guyonnet, D., Tournassat, C., Coelho, D., 2009. Na^+ and HTO diffusion in compacted bentonite: Effect of surface chemistry and related texture. *J. Hydrol.* 370, 9–20.

Melkior, T., Yahiaoui, S., Motellier, S., Thoby, D., Tevissen, E., 2005. Cesium sorption and diffusion in Bure mudrock samples. *Appl. Clay Sci.* 29, 172–186.

Melkior, T., Yahiaoui, S., Thoby, D., Motellier, S., Barthes, V., 2007. Diffusion coefficients of alkaline cations in Bure mudrock. *Phys. Chem. Earth, Parts A/B/C* 32, 453–462.

Molera, M., 2002. On the sorption and diffusion of radionuclides in Bentonite Clay. Ph. D. thesis, Royal Institute of Technolgy, Stockholm.

Molera, M., Eriksen, T., 2002. Diffusion of $^{22}Na^+$, $^{85}Sr^{2+}$, $^{134}Cs^+$ and $^{57}Co^{2+}$ in bentonite clay compacted to different densities: experiments and modeling. *Radiochim. Acta* 90, 753–760.

Molera, M., Eriksen, T., Jansson, M., 2003. Anion diffusion pathways in bentonite clay compacted to different dry densities. *Appl. Clay Sci.* 23, 69–76.

Motellier, S., Devol-Brown, I., Savoye, S., Thoby, D., Alberto, J.-C., 2007. Evaluation of tritiated water diffusion through the Toarcian clayey formation of the Tournemire experimental site (France). *J. Contam. Hydrol.* 94, 99–108.

Muurinen, A., Penitä-Hiltunen, P., Rantanen, J., 1986. Diffusion Mecflanisms of Srrontium and Cesium in Compacrtd Sodium Bentonite. In: *MRS Proceedings*. Cambridge Univ Press, p. 803.

Muurinen, A. 1990. Diffusion of uranium in compacted sodium bentonite. Engineering Geology 28 (3-4): 359-367.

Nakajima, M., Kozaki, T., Kato, H., Sato, S., Ohashi, H., 1997. The dependence of the diffusion coefficients of 3H and Cs on grain size in compacted montmorillonite. In: *MRS Proceedings*. Cambridge Univ Press, p. 947.

Nakashima, Y., 2000. The use of X-ray CT to measure diffusion coefficients of heavy ions in water-saturated porous media. *Eng. Geol.* 56, 11–17.

Nakashima, Y., 2002. Diffusion of H_2O and I^- in expandable mica and montmorillonite gels: contribution of bound H_2O. *Clays Clay Miner.* 50, 1–10.

Nakashima, Y., 2003. Diffusivity measurement of heavy ions in Wyoming montmorillonite gels by X-ray computed tomography. *J. Contam. Hydrol.* 61, 147–156.

Nakashima, Y., 2006. H_2O self-diffusion coefficient of water-rich MX80 bentonite gels. *Clay Miner.* 41, 659–668.

Nakashima, Y., Mitsumori, F., 2005. H_2O self-diffusion restricted by clay platelets with immobilized bound H_2O layers: PGSE NMR study of water-rich saponite gels. *Appl. Clay Sci.* 28, 209–221.

NEA, 2009. Mobile fission and activation products in nuclear waste disposal. NEA Report No. 6310, NEA, OECD (Nuclear Energy Agency, Organisation for Economic Co-operation and Development).

Neuzil, C.E., 1986. Groundwater flow in low-permeability environments. *Water Resour. Res.* 22, 1163–1195.

Neuzil, C.E., 1994. How permeable are clays and shales? *Water Resour. Res.* 30, 145–150.

Neuzil, C.E., 2013. Can shale safely host US nuclear waste? *EOS, Trans. Am. Geophys. Union* 94, 261–262.

Nye, P.H., 1980. Diffusion of ions and uncharged solutes in soils and soil clays. *Adv. Agron.* 31, 225–272.

Oscarson, D.W., Dixon, D.A., Hume, H.B., 1996. Mass transport through defected bentonite plugs. *Appl. Clay Sci.* 11, 127–142.

Pacala, S., Socolow, R., 2004. Stabilization wedges: solving the climate problem for the next 50 years with current technologies. *Science* 305, 968–972.

Pekala, M., D. K. A. Jan, H. N. Waber, T. Gimmi and P. Alt-Epping 2009. Transport of U-234 in the Opalinus Clay on centimetre to decimetre scales. Applied Geochemistry 24 (1): 138-152.

Pekala, M., J. D. Kramers and H. N. Waber 2010. $^{234}U/^{238}U$ activity ratio disequilibrium technique for studying uranium mobility in the Opalinus Clay at Mont Terri, Switzerland. Applied Radiation and Isotopes 68 (6): 984-992.

Rutqvist, J., Steefel, C., Davis, J., Bourg, I., Tinnacher, R., Galindez, J., Holmboe, M., Birkholzer, J., Liu, H.H. Investigation of Reactive Transport and Coupled THM Processes in EBS: FY12 Report, Lawrence Berkeley National Laboratory, DOE Used Fuel Disposition Campaign, FCRD-UFD-2012-000125. (2012).

Rutqvist, J., Davis, J., Zheng, L., Vilarrasa, V., Houseworth, J., Birkholzer, J., Investigation of Reactive Coupled THM Processes and Reactive Transport: FY14 Report, Lawrence Berkeley National Laboratory, DOE Used Fuel Disposition Campaign, FCRD-UFD-2014-000497. (2014).

Sato, H., Ashida, T., Kohara, Y., Yui, M., Sasaki, N., 1992. Effect of dry density on diffusion of some radionuclides in compacted sodium bentonite. *J. Nucl. Sci. Technol.* 29, 873–882.

Sato, H., Miyamoto, S., 2004. Diffusion behaviour of selenite and hydroselenide in compacted bentonite. *Appl. Clay Sci.* 26, 47–55.

Sato, H., Suzuki, S., 2003. Fundamental study on the effect of an orientation of clay particles on diffusion pathway in compacted bentonite. *Appl. Clay Sci.* 23, 51–60.

Savoye, S., Goutelard, F., Beaucaire, C., Charles, Y., Fayette, A., Herbette, M., Larabi, Y., Coelho, D., 2011. Effect of temperature on the containment properties of argillaceous rocks: The case study of Callovo–Oxfordian claystones. *J. Contam. Hydrol.* 125, 102–112.

Savoye, S., Page, J., Puente, C., Imbert, C., Coelho, D., 2010. New experimental approach for studying diffusion through an intact and unsaturated medium: a case study with Callovo-Oxfordian argillite. *Env. Sci. Tech.* 44, 3698–3704.

SKB, 2011. Long-term safety for the final repository for spent nuclear fuel at Forsmark. Main report of the SR-Site project. Volume I. SKB - TR-11-01.

Suzuki, S., Sato, H., Ishidera, T., Fujii, N., 2004. Study on anisotropy of effective diffusion coefficient and activation energy for deuterated water in compacted sodium bentonite. *J. Contam. Hydrol.* 68, 23–37.

Tachi, Y., Yotsuji, K., 2014. Diffusion and sorption of Cs^+, Na^+, I^- and HTO in compacted sodium montmorillonite as a function of porewater salinity: Integrated sorption and diffusion model. *Geochim. Cosmochim. Acta* 132, 75–93.

Tokunaga, T. K., J. M. Wan, J. Pena, S. R. Sutton and M. Newville 2004. Hexavalent uranium diffusion into soils from concentrated acidic and alkaline solutions. Environmental Science & Technology 38 (11): 3056-3062.

Van Loon, L.R., Baeyens, B., Bradbury, M.H., 2005a. Diffusion and retention of sodium and strontium in Opalinus clay: Comparison of sorption data from diffusion and batch sorption measurements, and geochemical calculations. *Appl. Geochem.* 20, 2351–2363.

Van Loon, L.R., Glaus, M.A., Müller, W., 2007. Anion exclusion effects in compacted bentonites: Towards a better understanding of anion diffusion. *Appl. Geochem.* 22, 2536–2552.

Van Loon, L.R., Müller, W., Iijima, K., 2005b. Activation energies of the self-diffusion of HTO, 22Na+ and 36Cl- in a highly compacted argillaceous rock (Opalinus Clay). *Appl. Geochem.* 20, 961–972.

Van Loon, L.R., Soler, J.M., Bradbury, M.H., 2003a. Diffusion of HTO, $^{36}Cl^-$ and $^{125}I^-$ in Opalinus Clay samples from Mont Terri: Effect of confining pressure. *J. Contam. Hydrol.* 61, 73–83.

Van Loon, L.R., Soler, J.M., Jakob, A., Bradbury, M.H., 2003b. Effect of confining pressure on the diffusion of HTO, 36Cl- and 125I- in a layered argillaceous rock (Opalinus Clay): diffusion perpendicular to the fabric. *Appl. Geochem.* 18, 1653–1662.

Van Loon, L.R., Soler, J.M., Muller, W., Bradbury, M.H., 2004a. Anisotropic diffusion in layered argillaceous rocks: a case study with Opalinus Clay. *Env. Sci. Tech.* 38, 5721–5728.

Van Loon, L.R., Wersin, P., Soler, J.M., Eikenberg, J., Gimmi, T., Hernan, P., Dewonck, S., Savoye, S., 2004b. In-situ diffusion of HTO, ^{22}Na$^+$, Cs$^+$ and I$^-$ in Opalinus Clay at the Mont Terri underground rock laboratory. *Radiochim. Acta* 92, 757–763.

Van Schaik, J., Kemper, W., 1966. Chloride diffusion in clay-water systems. *Soil Sci. Soc. Am. J.* 30, 22–25.

Wang, X., Liu, X., 2004. Effect of pH and concentration on the diffusion of radiostrontium in compacted bentonite—a capillary experimental study. *Appl. Radiat. Isot.* 61, 1413–1418.

Wang, X., Tan, X., Chen, C., Chen, L., 2005. The concentration and pH dependent diffusion of ^{137}Cs in compacted bentonite by using capillary method. *J. Nucl. Mater.* 345, 184–191.

Wang, X., Tao, Z., 2004. Diffusion of ^{99}TcO4$^-$ in compacted bentonite: Effect of pH, concentration, density and contact time. *J. Radioanal. Nucl. Chem.* 260, 305–309.

Wang, X.K., 2003. Diffusion of ^{137}Cs in compacted bentonite: Effect of pH and concentration. *J. Radioanal. Nucl. Chem.* 258, 315–319.

Wersin, P., Soler, J.M., Van Loon, L., Eikenberg, J., Baeyens, B., Grolimund, D., Gimmi, T., Dewonck, S., 2008. Diffusion of HTO, Br$^-$, I$^-$, Cs$^+$, ^{85}Sr^{2+} and ^{60}Co^{2+} in a clay formation: Results and modelling from an in situ experiment in Opalinus Clay. *Appl. Geochem.* 23, 678–691.

Wittebroodt, C., Savoye, S., Gouze, P., 2008. Influence of initial iodide concentration on the iodide uptake by the argillite of Tournemire. *Phys. Chem. Earth, Parts A/B/C* 33, 943–948.